WILEY-BLACKWELL

Cladistics (2019) 1–18

Cladistics

10.1111/cla.12367

A total evidence analysis of the phylogeny of hatchet-faced treefrogs (Anura: Hylidae: *Sphaenorhynchus*)

Katyuscia Araujo-Vieira[a], Boris L. Blotto[a,b], Ulisses Caramaschi[c], Celio F. B. Haddad[d], Julián Faivovich[a,e,*] and Taran Grant[b,*]

[a]*División Herpetología, Museo Argentino de Ciencias Naturales "Bernardino Rivadavia"-CONICET, Ángel Gallardo 470, Buenos Aires, C1405DJR, Argentina;* [b]*Departamento de Zoologia, Instituto de Biociências, Universidade de São Paulo, São Paulo, São Paulo, 05508-090, Brazil;* [c]*Departamento de Vertebrados, Museu Nacional, Universidade Federal do Rio de Janeiro, Quinta da Boa Vista, São Cristóvão, Rio de Janeiro, Rio de Janeiro, 20940-040, Brazil;* [d]*Departamento de Zoologia and Centro de Aquicultura (CAUNESP), Instituto de Biociências, Universidade Estadual Paulista, Avenida 24A, 1515, Bela Vista, Rio Claro, São Paulo, 13506–900, Brazil;* [e]*Departamento de Biodiversidad y Biología Experimental, Facultad de Ciencias Exactas y Naturales, Universidad de Buenos Aires, Buenos Aires, Argentina*

Accepted 14 November 2018

Abstract

The Neotropical hylid genus *Sphaenorhynchus* includes 15 species of small, greenish treefrogs widespread in the Amazon and Orinoco basins, and in the Atlantic Forest of Brazil. Although some studies have addressed the phylogenetic relationships of the genus with other hylids using a few exemplar species, its internal relationships remain poorly understood. In order to test its monophyly and the relationships among its species, we performed a total evidence phylogenetic analysis of sequences of three mitochondrial and three nuclear genes, and 193 phenotypic characters from all species of *Sphaenorhynchus*. Our results support the monophyly of *Sphaenorhynchus* with molecular and phenotypic evidence, with *S. pauloalvini* as the earliest diverging taxon, followed by *S. carneus*, as the sister taxon of all remaining species of the genus. We recognize three species groups in *Sphaenorhynchus* (the *S. lacteus*, *S. planicola* and *S. platycephalus* groups), to facilitate its taxonomic study; only three species (*S. carneus*, *S. pauloalvini* and *S. prasinus*) remain unassigned to any group. Sequence data were not available for only two species (*S. bromelicola* and *S. palustris*) for which we scored phenotypic data; wildcard behaviour was detected only in *S. bromelicola* nested inside the *S. platycephalus* group. On the basis of the resulting phylogenetic hypothesis, we discuss the evolution of oviposition site and a number of phenotypic characters that could be associated with heterochronic events in the evolutionary history of this group.

Introduction

Knowledge on the phylogenetic relationships of hylid frogs has increased qualitatively in the last 13 years. There are densely sampled hypotheses for several groups at different taxonomic levels (e.g. Phyllomedusinae, Cophomantini, Hylini, *Osteocephalus*, *Pseudis*; Faivovich et al., 2010; Jungfer et al., 2013; Pinheiro et al., 2019; Faivovich et al., 2018). Nevertheless, the internal relationships of the South American hatchet-faced treefrogs, *Sphaenorhynchus*, remain poorly known.

Sphaenorhynchus comprises 15 species of small, greenish treefrogs. Three species are widespread in the Amazon and Orinoco basins, including *S. carneus*, *S. dorisae* and *S. lacteus*, the last species also occurring in Trinidad (Kenny, 1969; as *Hyla orophila*) and northeastern Brazil (states of Maranhão and Piauí; La Marca et al., 2010; Caramaschi et al., 2009; Benício et al., 2011). The other 12 species occur in the Atlantic Forest of southeastern Brazil, from Pernambuco in the north to northern Rio Grande do Sul in the south, including *S. botocudo*, *S. bromelicola*, *S. cammaeus*,

*Corresponding authors.
E-mail address: julian@macn.gov.ar; taran.grant@ib.usp.br

S. canga, *S. caramaschii*, *S. mirim*, *S. palustris*, *S. pauloalvini*, *S. planicola*, *S. platycephalus*, *S. prasinus* and *S. surdus*. Adults of *Sphaenorhynchus* generally inhabit ponds in open areas and forest edges where males vocalize while perched on the floating vegetation or partially submerged in the water, or more rarely perched on bushes (e.g. Lutz and Lutz, 1938; Bokermann, 1973; Cruz and Peixoto, 1980; C.F.B. Haddad, pers. obs.). *Sphaenorhynchus dorisae*, *S. lacteus*, *S. surdus* and *S. caramaschii* attach their eggs to submerged vegetation (Rodriguez and Duellman, 1994; Toledo et al., 2007), whereas *S. pauloalvini* lays clutches on leaves overhanging water (Bokermann, 1973). *Sphaenorhynchus carneus* has been reported to lay clutches on leaves overhanging water (Bokermann, 1973) or in the water (Crump, 1974; W. Hödl, pers. comm.).

Most tadpoles of *Sphaenorhynchus* swim amid floating vegetation near the water surface, where they are associated with roots and under films of algae (*S. caramaschii*, *S. carneus*, *S. dorisae*, *S. lacteus* and *S. planicola*; Cruz, 1973; Suárez-Mayorga and Lynch, 2001; Araujo-Vieira et al., 2015a). However, larvae of *S. prasinus* and *S. surdus* inhabit darker and deeper places, amidst aquatic vegetation at the bottom of the water bodies (Bokermann, 1973; Caramaschi, 2010).

The remarkable occurrence of sexually mature individuals with larval somatic morphology, such as a long tail, has been reported in *S. bromelicola*, *S. botocudo*, *S. mirim* and *S. palustris* (Bokermann, 1974; Haddad and Prado, 2005; Caramaschi et al., 2009). Larvae of *S. bromelicola* close to metamorphosis with mature oocytes, specimens in metamorphosis and newly metamorphosed males emitting calls and with testicles in spermatogenesis were reported by Bokermann (1974), who explained this shift in the timing of sexual maturity as the result of both accelerated sexual maturation and delayed metamorphosis.

The monophyly of *Sphaenorhynchus* has been universally supported in recent analyses (Faivovich et al., 2005; Wiens et al., 2006, 2010; Pyron and Wiens, 2011; Pyron, 2014; Duellman et al., 2016), and several putative morphological synapomorphies have been suggested for the genus. Duellman and Wiens (1992) studied six species (*S. bromelicola*, *S. carneus*, *S. dorisae*, *S. lacteus*, *S. platycephalus* and *S. planicola*) and suggested 11 putative synapomorphies (mainly osteological), such as the posterior ramus of pterygoid absent and the postorbital process of maxilla reduced, not in contact with quadratojugal. Faivovich et al. (2005) also suggested as putative synapomorphies for *Sphaenorhynchus* the differentiation of the m. *intermandibularis* into a small apical supplementary element (see Tyler, 1971), the extreme development of the m. *interhyoideus*, the deposition of iridophores on the parietal peritoneum, and myrmecophagous adult diet. Subsequently, Araujo-Vieira et al. (2015a), based on Faivovich et al.'s (2005) comments, proposed the nostril with fleshy flanges and anteriorly directed as additional putative synapomorphies of *Sphaenorhynchus*.

In terms of the position of *Sphaenorhynchus* in Hylinae, Faivovich et al. (2005) obtained *Sphaenorhynchus* as sister taxon of *Xenohyla* + *Dendropsophus*, with this clade being the sister taxon of *Lysapsus*, *Pseudis*, *Scarthyla* and *Scinax*, together forming the tribe Dendropsophini. Wiens et al. (2006, 2010) obtained *Sphaenorhynchus* as the sister taxon of *Scinax*—with poor support—with this clade being the sister taxon of *Dendropsophus*, *Lysapsus*, *Pseudis, Scarthyla* and *Xenohyla*, therefore recovering—again with poor support—the monophyly of Dendropsophini as done by Faivovich et al. (2005). Pyron and Wiens (2011), Pyron (2014) and Duellman et al. (2016) also obtained *Sphaenorhynchus* as the sister taxon of *Scinax* (sensu Faivovich, 2002; Faivovich et al., 2005), with poor support (bootstrap with raxML < 50%; Shimodaira–Hasegawa < 64%), but more distantly related to *Dendropsophus*, *Lysapsus*, *Pseudis*, *Scarthyla* and *Xenohyla*, implying the paraphyly of Dendropsophini.

In a recent reanalysis of hylid GenBank sequences, Duellman et al. (2016), restricted Dendropsophini (as Dendropsophinae) to *Dendropsophus* + *Xenohyla*, resurrected Pseudinae Fitzinger 1843 for *Scarthyla*, *Lysapsus* and *Pseudis*, and erected the new subfamily Scinaxinae for *Scinax* + *Sphaenorhynchus*, a poorly supported clade with 49% bootstrap support in their analysis. In a recent molecular phylogenetic analysis of Hylini, Faivovich et al. (2018) discussed the problem of recognizing a subfamily (Scinaxinae) for a clade with unstable relationships and chose to restrict Scinaxini to *Scinax*, erect the tribe Sphaenorhynchini for *Sphaenorhynchus*, and recognize Dendropsophini for *Dendropsophus* + *Xenohyla*, and Pseudini for *Scarthyla*, *Lysapsus* and *Pseudis*.

Although previous studies have identified putative synapomorphies that support the monophyly of *Sphaenorhynchus*, the taxonomic distribution of these character-states is largely unknown. To date, analyses have included at most three species (*S. dorisae*, *S. lacteus* and *S. platycephalus*; the latter as *S. orophilus*; see Araujo-Vieira et al., 2018), and the relationships of the remaining species have not been studied in a quantitative phylogenetic framework. Given these limitations, in this paper we present a total evidence phylogenetic analysis of *Sphaenorhynchus*, with the goals of (i) testing the monophyly of *Sphaenorhynchus*; (ii) testing the relationships between the species of the genus; and (iii) studying the evolution of some morphological and reproductive biology characters in light of the resulting phylogenetic hypothesis.

Materials and methods

Taxon sampling

All known species of *Sphaenorhynchus* were included in the analysis. In order to test the monophyly of *Sphaenorhynchus*, outgroups were selected on the basis of the phylogenetic hypotheses of Faivovich et al. (2005), Wiens et al. (2010), Pyron and Wiens (2011), Pyron (2014) and Duellman et al. (2016), constrained by two criteria: (i) availability of tissues or sequences on GenBank and (ii) availability of specimens for morphological studies. Specifically, our outgroup sample includes *Dendropsophus elegans* (*D. leucophyllatus* group), *D. microps* (*D. parviceps* group), *D. minutus* (*D. minutus* group), *D. sanborni* (*D. microcephalus* group), *Pseudis minuta*, *Scarthyla goinorum*, and *Scinax alter* and *Sci. fuscovarius* (*Sci. ruber* clade), *Sci. catharinae* and *Sci. perpusillus* (*Sci. catharinae* clade), and *Xenohyla truncata*; the trees were rooted with *Phyllodytes luteolus*. Supplemental information Appendices S1 and S2 include a complete list of studied specimens. Institutional collection abbreviations follow Sabaj (2016).

Molecular character sampling

The mitochondrial DNA sequences used for the phylogenetic analyses include portions of *cytochrome b* (*cytb*, 385 bp), the ribosomal genes *12S*, $tRNA^{Val}$ and *16S* (~2450 bp), and a fragment including the complete downstream section of the *16S* gene, the intervening $tRNA^{Leu}$, NADH dehydrogenase subunit 1 and $tRNA^{Ile}$ (~1250 bp), giving a total of ~4085 bp of the mitochondrial genome. The nuclear protein-coding gene sequences include portions of recombination activating gene 1 (*RAG1*, 428 bp), rhodopsin (316 bp) and tyrosinase (532 bp) comprising 1276 bp of the nuclear genome. We complemented our new data with DNA sequences from Faivovich et al. (2005) and Wiens et al. (2006) available on GenBank (see Appendix S1). The final dataset includes ≈ 217 800 bp, with 717–5440 bp ($\bar{x}$ 4033 bp) per terminal.

Tissue samples were unavailable for *Sphaenorhynchus bromelicola* and *S. palustris*. The former is known only from the type locality "Fazenda Santo Onofre, 10 km à l'este de Maracás, Bahia, Brasil" and has not been collected since late 1965 (Bokermann, 1966, 1974). The latter was recently reported from Mucuri, State of Bahia, Brazil, 520 km SSE from the type locality (Lacerda and Moura, 2013); however, sequences of two of these specimens are identical to those of topotypes of *S. botocudo*, and we have been unable to differentiate the adult vouchers from topotypes of this species. As such, we tentatively consider the specimens referred to *S. palustris* by Lacerda and Moura (2013) to be *S. botocudo* (see Appendix S3 for further discussion).

Laboratory protocols

Whole cellular DNA was extracted from frozen and ethanol-preserved tissues (liver or muscle) using either phenol-chloroform extraction methods or the Qiagen DNeasy isolation kit. Primers used in PCR amplification and their citations are given in Appendix S4. PCR amplification was carried out in 25-μL reactions using 0.2 μL Taq (Fermentas). The PCR protocol consisted of an initial denaturation step of 3 min at 94 °C, 35 (for mitochondrial genes) or 45 (for nuclear genes) cycles of 30 s at 94 °C, 40 s at 48–62 °C, and 30–60 s at 72 °C, and a final extension step of 10–15 min at 72 °C. The PCR-amplified products were cleaned with 0.5 μL of Exonuclease plus 1 μL of alkaline phosphatase per 20 μL of reaction. Sequencing was done on an automatic sequencer ABI 3730XL (Applied Biosystems, Waltham, MA, USA) in both directions to check for potential errors and polymorphisms. The chromatograms obtained from the automated sequencer were read and contigs made using the sequence editing software Sequencher v.5.3 (Gene Codes, Ann Arbor, MI, USA) and edited the complete sequences with BioEdit (Hall, 1999). GenBank accession numbers are listed in Appendix S1.

Phenotypic character sampling

The terminology employed for external morphology follows Duellman (2001); Luna et al. (2018) for nuptial pad morphology; Trueb (1973, 1993) for cranial and postcranial osteology; Fabrezi (1992, 1993) for carpal and tarsal osteology; Trewavas (1933) for laryngeal morphology; Jurgens (1971) for nasal cartilage morphology; Burton (1996, 1998, 2004) and Faivovich (2002) for hand and foot myology; Tyler (1971), Trewavas (1933) and Horton (1982) for submandibular myology; and Altig and McDiarmid (1999) for external larval morphology. The states of characters 72, 74 and 76 for *Scinax catharinae* and *Sci. fuscovarius* were defined following Faivovich (2002, characters 11, 13 and 18). Osteological characters were coded from specimens that were cleared and double-stained with alcian blue and alizarin red (Taylor and Van Dyke, 1985). Larval characters were coded based on information taken from literature when larvae were unavailable for examination. When possible, one specimen of each sex from the type locality or close to it was used to code osteological and myological characters. However, in many cases only one specimen was available for these studies. Only males were examined to code characters of laryngeal morphology due to unavailability of females for most species and some females being

poorly stained with alcian blue. The final phenotypic dataset included 193 characters, 65 multistate, of which 41 were considered additive (see Appendices S5 and S6).

Phylogenetic analyses

Treatment of molecular and phenotypic characters. The ribosomal genes (*12S–16S*) and the protein-coding gene (*ND1*) were first broken into contiguous fragments of putative homology (Grant et al., 2006; Wheeler et al., 2006). The fragments were separated by inserting pound signs (#) exclusively in highly conserved regions identified by visualizing a preliminary MAFFT v.7 (Katoh and Standley, 2013; default parameters) similarity alignments using BioEdit (Hall, 1999).

Kluge and Grant (2006) argued that by globally minimizing the transformation events required to explain the variation of the character-states of the terminals studied, equally weighted parsimony analysis maximizes explanatory power. Therefore, in this study the molecular and phenotypic characters were treated under equal weights. The relation used to treat indels (insertions and deletions) and all substitutions was 1:1:1 (transition: transversion: unit indels). Matrix edition was done with Mesquite v.3.03 (Maddison and Maddison, 2015).

For total evidence analysis, we treated every specimen sequenced as a separate terminal for each ingroup species. Then, we duplicated the morphological entries for the species for each molecular terminal—that is, each conspecific terminal was given identical entries in the phenotypic matrix, following the arguments of Grant et al. (2006). This process was not extrapolated to the outgroup species; for these, we fused putatively conspecific specimens into a single polymorphic terminal—that is, we combined the morphological entries and different loci from different conspecific specimens into a single terminal (for outgroup sequences, see Appendix S1). Loci not sequenced for particular terminals due to primer failure or unavailability on GenBank were treated as missing data. Multistate characters were considered either as additive or nonadditive; additive characters were coded according to Hawkins et al. (1997) and Strong and Lipscomb (1999). Species-level phenotypic polymorphisms were coded as ambiguities.

Choice of phylogenetic method. The optimality criterion used to identify the preferred phylogenetic hypothesis was parsimony, a nonstatistical, nonparametric, evidentially conservative approach to scientific inference that maximizes explanatory power by minimizing both the quantity of evolutionary events and assumptions about the process of character evolution that are required to explain the evidence (Kluge and Grant, 2006; Grant and Kluge, 2009; for further discussion see Padial et al., 2014).

On the basis of the arguments of Padial et al. (2014; see also Kluge and Grant, 2006; Grant and Kluge, 2009), we employed direct optimization (e.g. Sankoff, 1975; Wheeler, 1996; Varón and Wheeler, 2012, 2013) in the program POY v.5.1.1 (Wheeler et al., 2015), which tests hypotheses of nucleotide homology dynamically by optimizing unaligned DNA sequences directly onto alternative topologies (Kluge and Grant, 2006; Wheeler et al., 2006; Grant and Kluge, 2009) while simultaneously optimizing prealigned transformation series (e.g. morphology) as standard matrices.

Data analysis. We consider the results of the total evidence analysis to be the phylogenetic hypothesis that best explains the evidence, because the analysis of all available evidence maximizes explanatory power (Kluge, 1989; Grant and Kluge, 2003), and all discussion of character evolution and phenotypic synapomorphies is based on the results of total evidence analysis. Nevertheless, to test the effects of including terminals lacking an entire data partition (i.e. terminals scored only for molecular or phenotypic data), we performed independent analyses of three datasets: (i) molecular data only; (ii) phenotypic data only; and (iii) total evidence (molecular and phenotypic data).

The molecular-only dataset (MD) included DNA sequences for 53 terminals (12 outgroup and 41 ingroup; Appendix S1). The phenotypic dataset (PD) included 27 terminals (12 outgroup and 15 ingroup, see Appendices S2 and S5). The total evidence analysis (TE) included 55 terminals, including all 53 MD terminals combined with phenotypic data as described above, plus two PD terminals (*Sphaenorhynchus bromelicola* and *S. palustris*) for which DNA sequences were not available.

The PD matrix was analysed using TNT v.1.5 (Goloboff et al., 2008; Goloboff and Catalano, 2016; equal costs for all transformations). Shortest trees were found by performing either 1000 random addition sequences (RAS), retaining 10 trees per replicate, and then submitting them to a round of tree bisection and reconnection (TBR) branch swapping, or a driven search with the option "New Technology Search." This search option includes the algorithms Ratchet (Nixon, 1999), Tree Drifting (Goloboff, 1999), Sectorial Searches (Goloboff, 1999) and Tree Fusing (Goloboff, 1999). For this driven search, we used the default options for these algorithms, and the maximum-parsimony trees were requested to be hit 1000 times. The resulting trees were submitted to a round of TBR branch swapping. All searches were done under

the collapsing option "minimum length", which collapses every node whose minimum length is 0.

Total evidence and molecular-only analyses comprised several steps. First, using the standard direct optimization algorithm (Wheeler, 1996), we ran two 2-h searches using 768 CPUs (=3072 CPU-hours) using the command "search", which implements a driven search composed of random addition sequence Wagner builds, Subtree Pruning and Regrafting (SPR) and Tree Bisection and Reconnection (TBR), branch swapping (RAS + swapping; Goloboff, 1996), Parsimony Ratcheting (Nixon, 1999) and Tree Fusing (Goloboff, 1999), and alternates between the specified optimization algorithm (standard direct optimization in this case) and static-approximation, which searches using the implied alignment of the best tree in memory. Given the high time complexity of direct optimization (Varón and Wheeler, 2012), a common procedure to accelerate analyses is to treat equal-length sequences as prealigned, static-homology matrices (e.g. Faivovich et al., 2010). Insofar as the resulting speed-up enables a greater tree-space to be explored in a given amount of time, this can result in more parsimonious trees. As such, we analysed the total evidence and molecular-only datasets with *cytb* and nuclear genes treated as both prealigned and unaligned sequences.

Second, we swapped the best trees from the first analyses using the approximate iterative pass algorithm (Wheeler, 2003a) and generated the matrix version of the alignment (i.e. implied alignment; Wheeler, 2003b). Third, to verify the length reported by POY and search for better and/or additional trees given the implied alignment, we performed driven search of the implied alignment in TNT v.1.5 (Goloboff et al., 2008; Goloboff and Catalano, 2016; equal costs for all transformations, gaps treated as fifth state), stopping when the stable consensus was reached 10 times (tnt command: xmult = level 5 chklevel 5 consense 10).

Once we identified the most parsimonious trees (MPTs), we estimated clade support (Grant and Kluge, 2008) for the clades present in the optimal trees by calculating Goodman–Bremer values (GB; Goodman et al., 1982; Bremer, 1988; Grant and Kluge, 2008) in TNT v.1.5 (Goloboff et al., 2008; Goloboff and Catalano, 2016) using the implied alignment and the parameters specified in the bremer.run macro (for details see Goloboff et al., 2008; macro available at http://www.lillo.org.ar/phylogeny/tnt/). Although shorter suboptimal trees might be found by calculating the optimal tree-alignment for each visited topology, the time requirements would be prohibitive unless searches were extremely superficial. Further, Padial et al. (2014) found that using the implied alignment to estimate support overestimates GB values less than when GB is calculated using a MAFFT similarity-alignment. Parsimony jackknife absolute frequencies (Farris et al., 1996) were calculated in TNT v.1.5 (Goloboff et al., 2008; Goloboff and Catalano, 2016) using a MAFFT similarity-alignment and driven search with the option "New Technology Search" requesting 10 hits with driven searches under search level 15, for a total of 1000 replicates.

All POY analyses were run on Ace, a high-performance computing cluster composed of 12 quad-socket AMD Opteron 6376 16-core 2.3-GHz CPU, 16 MB cache, 6.4 GT/s compute nodes (= 768 cores total), eight with 128 GB RAM DDR3 1600 MHz (16 × 8 GB), two with 256 GB (16 × 16 GB), and two with 512 GB (32 × 16 GB) and QDR 4× InfiniBand (32 GB/s) networking. Results were visualized using Mesquite v.3.03 (Maddison and Maddison, 2015). Lists of phenotypic synapomorphies were generated with YBYRÁ (Machado, 2015) using TNT. YBYRÁ categorizes character transformation events from any source of data given all possible optimization schemes in a set of trees. It proceeds by spawning trees and data matrix to TNT to compile synapomorphies using TNT's command "apo". Character-state transformations of a node were considered synapomorphies if they (i) were optimized unambiguously (without arbitrary selection of accelerated, ACCTRAN, or delayed optimization, DELTRAN) and (ii) were shared by all dichotomized most parsimonious trees. YBYRÁ generates colour-coded boxes to indicate if a synapomorphic character-state occurs only in the clade in question (nonhomoplastic) or also occurs in other clades (homoplastic), and if it is shared by all terminals of the clade (unique) or is subsequently transformed into one or more different states within the clade (nonunique).

Results

Phylogenetic analyses

The driven searches of MD performed 39 598 RAS + TBR, 394 867 rounds of tree fusing, and 22 935 rounds of ratcheting when *cytb* and nuclear loci were treated as prealigned; 33 840 RAS + TBR, 320 271 rounds of tree fusing, and 19 720 rounds of ratcheting when all data were subjected to direct optimization; driven searches of TE 37 769 RAS + TBR, 438 830 rounds of tree fusing, and 23 347 rounds of ratcheting when *cytb* and nuclear loci were treated as prealigned; and 31 889 RAS + TBR, 341 268 rounds of tree fusing and 19 920 rounds of ratcheting when all data subjected to direct optimization. Despite performing 14–22% more tree searching operations, trees were consistently longer when *cytb* and nuclear loci were treated as prealigned than when all DNA sequences were analysed under direct optimization, with the best scores being, respectively, 8804 and 8779

steps for MD, and 9601 and 9577 steps for TE. Swapping the best MD and TE trees under iterative pass further reduced the lengths to 8769 steps for MD and 9557 for TE. Driven searches of the implied alignments in TNT did not result in shorter trees, but they did increase the number of most parsimonious trees to four for MD and nine for TE.

The TE parsimony analysis recovered *Sphaenorhynchus* as a well-supported monophyletic group (jackknife support = 100%; GB = 90), sister taxon of *Dendropsophus* + *Xenohyla* (Fig. 1). *Sphaenorhynchus pauloalvini* is the earliest diverging taxon of the genus, followed by *S. carneus*, sister taxon (jackknife support = 100%; GB = 48) of all remaining species of *Sphaenorhynchus*.

The interspecific relationships are well supported in general (jackknife support > 90%; GB 10–48), although the positions of *S. dorisae* + *S. lacteus* and *S. prasinus* (jackknife support < 50%; GB = 10 and 17) and some internal clades of Atlantic Forest species are poorly supported (jackknife support < 65%; GB = 1–3). The conflicts among topologies are restricted to the internal relationship among *S. bromelicola*, *S. canga*, *S. platycephalus*, *S. surdus*, and *S. botocudo* + *S. palustris* (see Fig. 1). The Amazonian species (*S. carneus*, *S. dorisae* and *S. lacteus*) are not recovered as a monophyletic group; *S. lacteus* and *S. dorisae* form a well-supported clade (jackknife support = 100%; GB = 31) nested among species of the Atlantic Forest.

The PD parsimony analysis resulted in 14 MPTs of 751 steps. Similar to the TE and MD analyses, this result recovered *Sphaenorhynchus* as a well-supported monophyletic taxon, *S. pauloalvini* as the sister taxon of all other species in the genus, and *S. carneus* as the sister taxon of the remaining *Sphaenorhynchus* (see Fig. S1). The interspecific relationships of *Sphaenorhynchus* are similar in the MD and TE analyses, differing solely in that the MD analysis does not include *S. bromelicola* and *S. palustris* (for which there are no DNA sequences; see Fig. S2). Nevertheless, all conflict between the 14 MPTs in the PD analysis is restricted to the internal relationship of the sister group of *S. carneus*, which involves the positions of *S. bromelicola*, *S. cammaeus*, *S. canga* and *S. platycephalus* with respect to the remaining species inside that clade (see Fig. S1). The interspecific relationships are poorly supported in general (jackknife support < 66%; GB = 2–3) in the PD analysis; exceptions are the position of *S. carneus* in relation to the other species, the sister taxon of *S. carneus*, and *S. mirim* + *S. planicola* that are well supported (jackknife support > 85%; GB = 6–7); and *S. botocudo* + *S. palustris* and *S. caramaschii* + *S. surdus*, which are moderately supported (jackknife support = 68% and 73%; GB = 2–3). Also, in contrast with the TE analysis, *S. lacteus* and *S. dorisae* do not form a clade in the PD analysis.

Discussion

Topological effects of including terminals with missing data

The main concern about including terminals with a large amount of missing data in total evidence analyses is that those terminals might exhibit wildcard behaviour (Nixon and Wheeler, 1992). However, the amount of missing data *per se* is not enough for the terminals to behave as wildcards. Unpredictability of the relationship between amount of evidence and wildcard behaviour was demonstrated by previous studies (e.g. Kearney, 2002; Grant and Kluge, 2003; Kearney and Clark, 2003; Grant et al., 2017).

Our TE dataset included 55 terminals, with two terminals that lack molecular data—*S. bromelicola* and *S. palustris*—and therefore the effect of putative wildcard behaviour focuses on these terminals. The inclusion of *S. bromelicola* in the TE analyses appears to be responsible for the incongruence among primary topologies, because it could be sister taxon of *S. canga*, *S. platycephalus*, or *S. botocudo* + *S. palustris*. This terminal contributed to the corresponding polytomies and low support within the clade including *S. botocudo*, *S. canga*, *S. palustris*, *S. platycephalus* and *S. surdus*. The exclusion of *S. bromelicola* results in moderately to well-supported (jackknife support > 77%) resolved interspecific relationships within this clade in the strict consensus. By contrast, the position of *S. palustris* was consistent among the optimal topologies. This terminal is sister taxon of *S. botocudo* with 76% jackknife support in the TE analysis.

As mentioned before, the interspecific relationships of *Sphaenorhynchus* are similar in the MD and TE analyses, differing solely in that the MD analysis does not include *S. bromelicola* and *S. palustris* (Fig. S2). In the PD analysis, the internal relationships of the sister group of *S. carneus* are different from those in the TE analyses; exceptions are the position of *S. botocudo* as sister taxon of *S. palustris*, and *S. mirim* as sister taxon of *S. planicola*, which are consistent in both analyses. The position of *S. palustris* is moderately supported in the PD analysis (jackknife support = 73%, GB = 3) similar to the TE analysis (jackknife support = 76%, GB = 3). In contrast, the position of *S. bromelicola* is unresolved in both PD and TE analyses, but in the TE analysis it is nested inside a well-supported group (jackknife support = 98%, GB = 11) with all other morphologically similar species of the Atlantic Forest, a relationship that was not supported in the PD analysis (compare Fig. 1 with Fig. S1). Therefore, our results indicate that only one of the terminals with missing data behaved as a wildcard, but its impact on our inference

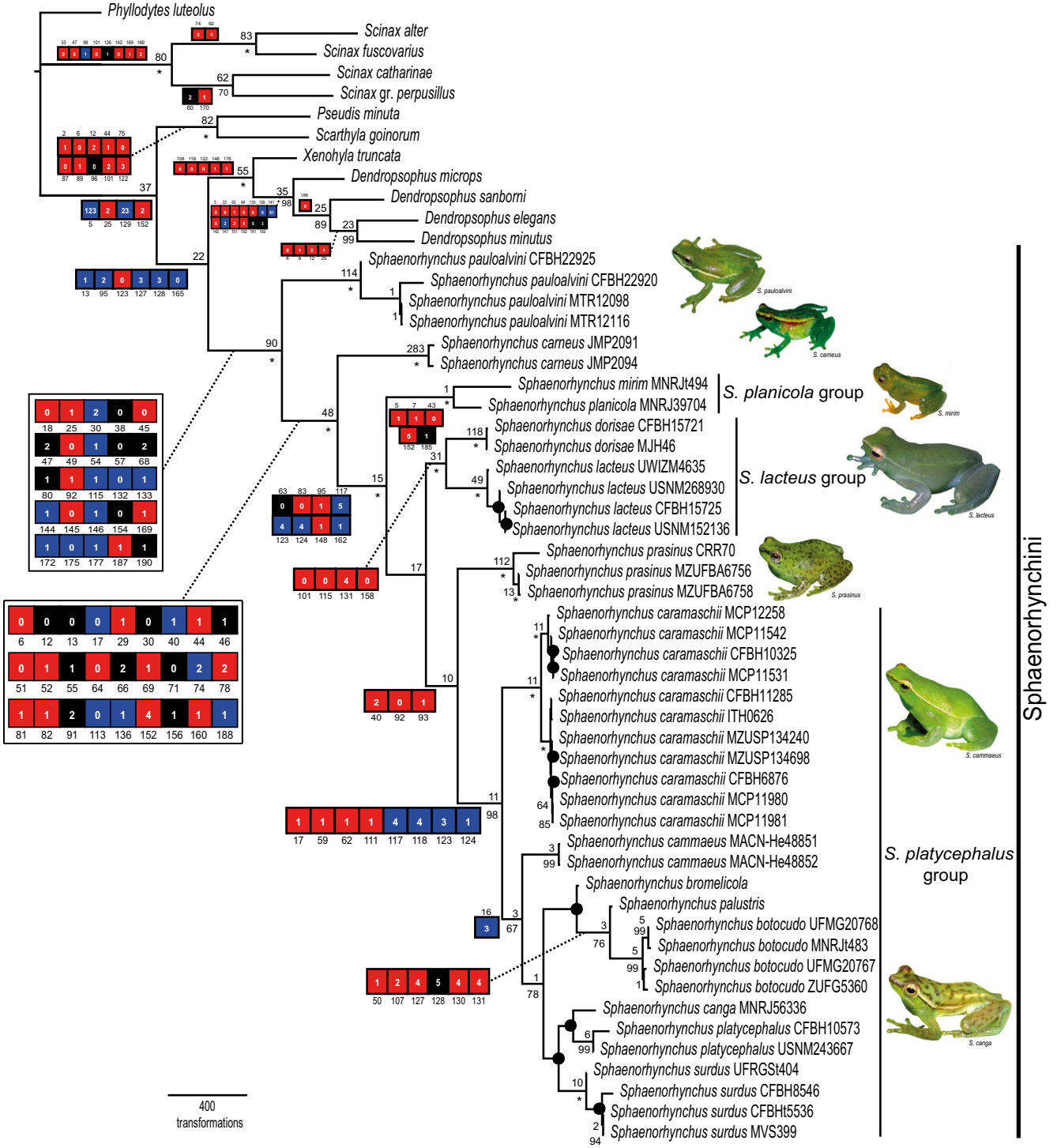

Fig. 1. Phylogenetic relationships of *Sphaenorhynchus* as recovered in one of the nine most parsimonious trees obtained from the analysis of total evidence (TE) with direct optimization (length 9557 steps) under equal weights for all transformations. Black circles indicate nodes that collapse in the strict consensus. Values above nodes are Goodman–Bremer support. Values below nodes are parsimony jackknife support absolute frequencies estimated for the static alignment analysed with parsimony in TNT with gaps as fifth state. An asterisk (*) indicates groups with 100% for parsimony jackknife frequencies. Nodes lacking values have < 50% jackknife support. Nodes are labelled with unambiguously optimized phenotypic synapomorphies (black square = unique, nonhomoplastic; red square = unique, homoplastic; blue square = nonunique, homoplastic; character number below or above squares; derived character-states inside squares). Photos of I.J. Roberto (*S. cammaeus* and *S. prasinus*), F.S.F. Leite (*S. canga*), C.E. Costa-Campos (*S. carneus*), T. Grant (*S. lacteus*), J.L. Gasparini (*S. mirim*), and M.T. Rodrigues (*S. pauloalvini*).

is restricted to few interspecific relationships inside the sister group of *S. cammaeus*.

Sphaenorhynchus *monophyly and outgroup relationships*

The main goal of our analysis was to provide a rigorous test of the monophyly of *Sphaenorhynchus* and its internal relationships, and not the relationships between *Sphaenorhynchus* and other hylids, given that previous studies have performed stronger tests of those relationships (Faivovich et al., 2005; Wiens et al., 2006; Duellman et al., 2016). However, some putatively shared morphological synapomorphies proposed for *Sphaenorhynchus* and outgroups deserve comment (Duellman and Wiens, 1992; Izecksohn, 1998; Faivovich et al., 2005). Contrary to Duellman and Wiens's (1992) hypothesis, the monophyly of *Scarthyla*, *Scinax* and *Sphaenorhynchus* is rejected in our results (see also Faivovich et al., 2005; Wiens et al., 2005, 2006; Duellman et al., 2016). However, Duellman and Wiens (1992) proposed three putative morphological synapomorphies for this group: (i) narrow sacral diapophyses (rounded, not strongly dilated), (ii) anteriorly inclined alary processes of the premaxillae and (iii) tadpole with large, laterally positioned eyes. The character-states of the sacral diapophyses were redefined by Faivovich (2002), who suggested that rounded or weakly expanded sacral diapophyses are a synapomorphy of *Scinax*. Subsequently, in a more comprehensive phylogenetic context, Faivovich et al. (2005) suggested that this character-state might be a synapomorphy of a more inclusive clade.

The optimization of sacral diapophysis expansion (our Ch. 95) and orientation of the premaxilla (our Ch. 19; orientation of the alary processes of the premaxilla sensu Duellman and Wiens, 1992) indicates that moderately expanded diapophyses (our Ch. 95.1) optimize as a synapomorphy of the sister taxon of *S. carneus*, with a transformation to unexpanded diapophyses in *S. mirim* (Ch. 95.0). The anteriorly directed premaxilla (our Ch. 19.0) optimizes ambiguously on the common ancestor of *Sphaenorhynchus* + (*Xenohyla* + *Dendropsophus*), a character-state shared with *Scarthyla goinorum*, *Scinax alter* and *Sci. perpusillus*. The size and the degree of lateralization of eyes did not present informative variation, because the eyes are ventrally visible (sensu Faivovich, 2002) in all larvae of *Sphaenorhynchus* examined and we were unable to objectively delimit character-states to characterize the size of eyes.

Izecksohn (1998) suggested that *Xenohyla* and *Sphaenorhynchus* share (i) reduced number of teeth in the jaw, (ii) relatively short urostyle, (iii) elongate and posteriorly directed transverse process of presacral vertebra IV, and (iv) the quadratojugal without contact with the maxilla. We did not score the relative length of the urostyle, but we have noticed that in *S. carneus* the urostyle is shorter than in other species of *Sphaenorhynchus* (see Appendix S7). *Xenohyla truncata* shares a 35–40% edentate maxilla (our Ch. 16.2) with *S. caramaschii*, *S. lacteus*, *S. prasinus* and *S. surdus*. However, the optimization of this character indicates that this character-state evolved independently in *Xenohyla* and these species of *Sphaenorhynchus*.

We considered the elongate and posteriorly directed transverse process of presacral vertebra IV as two independent characters, scored as (i) orientation and (ii) length of the transverse processes. In our observations, only the length of this process was variable (Ch. 91). As a result of our analyses, the elongate transverse process of presacral IV (Ch. 91.2; Fig. S12d) is an unique synapomorphy for the sister taxon of *S. pauloalvini*. *Xenohyla truncata*, in turn, presents a moderately long transverse process (Ch. 91.1), the plesiomorphic condition.

A quadratojugal without contact with the maxilla, according to our observations, is the result of two independent transformations: the posterior reduction of the maxilla (Ch. 13) and the anterior reduction of the quadratojugal (Ch. 22). For example, in *S. pauloalvini* both the maxilla (Ch. 13.1) and quadratojugal (Ch. 22.1) are moderately developed, whereas in *S. carneus* both the maxilla (Ch. 13.0) and quadratojugal (Ch. 22.0) are extremely reduced. Furthermore, these bones are not in contact due to the extreme (Ch. 13.0) and moderate (13.1) posterior reduction only the maxilla in other *Sphaenorhynchus* and *X. truncata*, respectively.

According to Barrio-Amorós et al. (2006), *Sphaenorhynchus*, *Scarthyla* and *Pseudis* share mineralized intercalary elements. In our analyses, the completely mineralized intercalary element (Ch. 101.2) is a synapomorphy of *Scarthyla* + *Pseudis*, with instances of homoplasy in *Dendropsophus minutus*, *D. sanborni*, *Sphaenorhynchus botocudo*, *S. caramaschii*, *S. mirim* and *S. pauloalvini*.

Sphaenorhynchus *internal relationships*

The monophyly of *Sphaenorhynchus* is well supported (jackknife support = 100%; GB = 90; Fig. 1) by molecular evidence and 25 phenotypic synapomorphies in the TE analysis (see Appendix A for the complete list of synapomorphies of *Sphaenorhynchus*), with *S. pauloalvini* being the sister taxon of all other species of the genus.

Our observations corroborate Faivovich et al. (2005) and Araujo-Vieira et al.'s (2015a) suggestions that the anteriorly directed larval nostril (Ch. 132.0) and larval nostril with fleshy flanges (Ch. 133.1) are synapomorphies of *Sphaenorhynchus*. Similarly, we corroborated Faivovich et al.'s (2005) suggestions that the presence of a differentiated m. *intermandibularis* with a well-

developed apical supplementary element (our Ch. 146.1; see Fig. S14) and the white parietal peritoneum (Ch. 190.1) are synapomorphies of *Sphaenorhynchus*. The apical element also is present in other species of hylids (e.g. *Acris crepitans* and *A. gryllus*) and Lophyohylini (e.g. *Osteopilus dominicensis* and *O. ocellatus*; Tyler, 1971; Trueb and Tyler, 1974), as is the white parietal peritoneum (e.g. *Aplastodiscus* and *Hyloscirtus bogotensis* group, *Boana punctata* group, some species in the *B. benitezi* and *B. pulchella* groups; Ruiz-Carranza and Lynch, 1982; Garcia et al., 2003; Faivovich et al., 2005, 2006), indicating that these are homoplastic in a broader phylogenetic context.

Duellman and Wiens (1992) studied six species of *Sphaenorhynchus* (*S. bromelicola*, *S. carneus*, *S. dorisae*, *S. lacteus*, *S. planicola* and *S. platycephalus*) and proposed 11 morphological synapomorphies for the genus: (i) posterior ramus of pterygoid absent; (ii) zygomatic ramus of squamosal absent or reduced to small knob; (iii) pars facialis of maxilla and alary process of premaxilla reduced; (iv) postorbital process of maxilla reduced, not in contact with quadratojugal; (v) palatine reduced to sliver or absent; (vi) pars externa plectri entering tympanic ring posteriorly (rather than dorsally); (vii) pars externa plectri round; (viii) hyale curved medially; (ix) coracoids and clavicles elongate; (x) transverse process of presacral vertebra IV elongate, oriented posteriorly; and (xi) prepollex ossified, bladelike. We divided characters (ii), (iii) and (ix) into two independent characters each (see Discussion of characters 24–25, 12 and 18, and 81–82, respectively, in Appendix S6).

Only three of Duellman and Wiens's (1992) synapomorphies are supported in our results: (ii; our Ch. 25.1), with instances of homoplasy in *Dendropsophus elegans* and *Pseudis minuta*; (iii; our Ch. 18.0), with instances of homoplasy in *D. elegans* and *D. sanborni* and (vii; our Ch. 47.2). Of the remaining character-states, (iii; our Ch.12.0), (iv; our Ch. 13.0), (viii; our Ch. 69.1) and (x; our Ch. 91.2), and modified (i; our Ch. 30.0), (v; our Ch. 40.1) and (ix; our Ch. 81.1–82.1) optimize as synapomorphies of the clade that comprises all species of *Sphaenorhynchus* except *S. pauloalvini* (Fig. 1).

There are three remaining transformations: character (ii; our Ch. 24.0), zygomatic ramus of squamosal absent optimizes as an autapomorphy of *Sphaenorhynchus carneus*, with an extremely short zygomatic ramus of squamosal (our Ch. 25.0) optimizing ambiguously for its sister taxon due to the absence of this process in *S. carneus*; character (vi; our Ch. 48.1) which optimizes ambiguously for *Sphaenorhynchus*, a character-state shared with *Pseudis minuta* and *Xenohyla truncata*; and the character (xi; our Ch. 98.0) that is plesiomorphic for *Sphaenorhynchus*.

The exceptional posterior development of the m. *interhyoideus* was suggested by Faivovich et al. (2005) to be a putative synapomorphy of *Sphaenorhynchus*. However, the transformation in which the posterior margin of the muscle reaches the m. *pectoralis esternalis* (Ch. 152.4) is a synapomorphy of all *Sphaenorhynchus* except *S. pauloalvini*.

Furthermore, based on previous reports for six species (*S. carneus*, *S. dorisae*, *S. lacteus*, *S. planicola*, *S. prasinus*, and *S. surdus*; Duellman, 1978; Rodriguez and Duellman, 1994; Parmalee, 1999; C.F.B. Haddad, pers. obs.) Faivovich et al. (2005) proposed that myrmecophagy is a likely synapomorphy of *Sphaenorhynchus*. Our study of stomach contents of *S. pauloalvini* (MNRJ 4323) revealed ants as well, corroborating that myrmecophagy is a putative synapomorphy of *Sphaenorhynchus*.

The differences that we found regarding the synapomorphies resulting from our analysis and several of those suggested by previous studies stem from the fact that *S. pauloalvini* had not been considered in other studies. Although *S. pauloalvini* presents a number of character-states that differ from those of other species of *Sphaenorhynchus* (see Appendices S5 and S6), all of our analyses indicate that it is the sister taxon of all remaining species of the genus, and so differences in the inferred phenotypic synapomorphies result from limitations in the taxonomic sampling of earlier studies. In Appendix A we provide an updated diagnosis of *Sphaenorhynchus* including all synapomorphies inferred from our results in addition to those discussed above.

The clade including all species of *Sphaenorhynchus* except *S. pauloalvini* is well supported (jackknife support = 100%; GB = 48) by molecular evidence and 27 phenotypic synapomorphies in the TE analysis (Fig. 1). Our analysis corroborates Araujo-Vieira et al.'s (2015a, b) suggestion that the presence of few enlarged marginal papillae (Ch. 136.1: marginal papillae about twice larger than the small papillae) on the oral disc is a synapomorphy of this clade. Another of its synapomorphies, the m. *petrohyoideus anterior* with an additional layer of fibres over the hyoid plate (Ch. 156.1) is known only in this genus among hylines (see Fig. S14c). Besides the synapomorphies mentioned above, some transformations are related to the absence or reduction of bones, including the extremely short posterior ramus of pterygoid, reduced to rudimentary bumps (Ch. 30.0), and the simple proximal portion of the *pars media plectri*, with a large gap between basal plate and operculum (Ch. 51.0).

In *Sphaenorhynchus* we recover three clades including species that are quite characteristic, and three species that we do not assign to any group, the early diverging *S. pauloalvini* and *S. carneus*, and *S. prasinus*. The clades that we recover include one with the small species from coastal lowlands in southeastern Brazil that we recognize as the *S. planicola* group (*S. mirim* and *S. planicola*; combined snout-to-vent

length (SVL) in males 15.7–24.1 mm; Lutz and Lutz, 1938; Caramaschi et al., 2009); the relatively large Amazonian species that we recognize as the *S. lacteus* group (*S. dorisae* and *S. lacteus*; combined SVL in males 26.0–41.0 mm, females 36.0–46.0 mm; Rodriguez and Duellman, 1994); and the clade including the medium-sized species of the Atlantic Forest, that we recognize as the *S. platycephalus* group (*S. botocudo*, *S. bromelicola*, *S. cammaeus*, *S. canga*, *S. caramaschii*, *S. palustris*, *S. platycephalus* and *S. surdus*; combined SVL in males 22.5–36.0 mm, females 20.0–33.0 mm; Lutz and Lutz, 1938; Bokermann, 1966; Heyer et al., 1990; Toledo et al., 2007; Caramaschi et al., 2009; Araujo-Vieira et al., 2015b; Roberto et al., 2017).

Cruz and Peixoto (1980) tentatively grouped *S. planicola* with *S. prasinus* on the basis of several larval similarities including total length, colour pattern, spiracle length and marginal papillae size. However, the monophyly of this clade is rejected in our analyses. Instead, *S. planicola* is sister taxon of *S. mirim*, which we recognize as the *S. planicola* group. The monophyly of this group is supported by molecular evidence and five phenotypic synapomorphies (jackknife support = 100%; GB = 1). Some phenotypic synapomorphies are the posterior extension of the fold of the m. *interhyoideus* surpassing the m. *pectoralis esternalis* (Ch. 152.5), the posterior-most extension of this muscle in *Sphaenorhynchus*, with instances of homoplasy in *Dendropsophus minutus* and *D. sanboni*, and the m. *extensor brevis superficialis digiti III* with an insertion on the third metatarsus (Ch. 185.1; Fig. S15d) as synapomorphy of this clade in our TE results (nonhomoplastic in the context of our analysis, but known to occur in several distantly related anurans such as *Pipa pipa* (Pipidae), *Chiromantis xerampelina* (Rhacophoridae), and *Phrynobatrachus kinangopensis* (Phrynobatrachidae), *Hyla meridionalis* (Hylinae), and several phyllomedusines; Dunlap, 1960; Burton, 2004).

The monophyly of the *S. lacteus* group is supported by molecular evidence and four phenotypic synapomorphies (jackknife support = 100%; GB = 31), including the light-coloured nuptial pads on Finger II in males (Ch. 115.0), with a single instance of homoplasy in *S. canga* and branch I of the m. *petrohyoideus posterior* inserted on the base of the posteromedial process of the hyoid (Ch. 158.0), with instances of homoplasy in *Dendropsophus minutus*, *Pseudis minuta* and *Scinax alter*.

The monophyly of the *S. platycephalus* group is supported by molecular evidence and eight phenotypic synapomorphies (jackknife support = 98%; GB = 11), with *S. caramaschii* as the earliest diverging taxon of this clade, followed by *S. cammaeus*. Some of these synapomorphies are as follows: maxilla overlapping the premaxilla (Ch. 17.1); dorsolateral white line present (Ch. 111.1), with instances of homoplasy in *Dendropsophus sanborni*, *Scinax alter* and *S. lacteus*; subcloacal ornamentation with a weak glandular dermal fold (Ch. 117.4); poorly developed and slightly crenulated dermal folds on tarsus (Ch. 123.3); and small, rounded or flattened tubercles on heel (Ch. 124.1). A notable synapomorphy of this clade is the presence of a cartilaginous lamina that extends from the cartilaginous branch to the inferior margin of the oblique cartilage (Ch. 62.1) with instances of homoplasy in *S. lacteus*, *S. pauloalvini* and species of *Dendropsophus* (see Fig. S9). See Appendix A for a complete diagnosis and characterization of the three species groups of *Sphaenorhynchus*.

Paedomorphosis and character evolution in Sphaenorhynchus

Bokermann (1974) reported that some tadpoles of *S. bromelicola* stage 41 of Gosner (1960) possess mature oocytes and well-developed testes. Furthermore, he reported newly metamorphosed individuals and individuals close to reducing the tail having well-developed oocytes or vocal sac—with some individuals even calling—and testes in spermatogenesis. These individuals are, at least in relation to development and fertility of gonads, able to reproduce. Bokermann (1974) suggested that there is acceleration in the time of the sexual maturity (peramorphosis sensu Reilly et al., 1997) together with a delay and irregular metamorphosis (paedomorphosis sensu Reilly et al., 1997). Also, although *S. bromelicola* is associated with unstable environments (temporary ponds), the presence of individuals in the same population with regular metamorphosis suggests that this precocity is not necessarily dependent on environmental factors (Bokermann, 1974).

Among species of *Sphaenorhynchus*, sexually mature individuals with a long tail (larval somatic morphology) have been reported for *S. botocudo*, *S. bromelicola*, *S. mirim* and *S. palustris* (Haddad and Prado, 2005; Caramaschi et al., 2009). These species do not form a clade in our TE results. Instead, the presence of a long tail in sexually mature individuals optimizes as a synapomorphy of *S. botocudo* + *S. palustris*, and autapomorphies of *S. bromelicola* and *S. mirim*. This occurrence might result from a deceleration in the process of tail resorption, because the ancestral condition is absence of long tails in sexually mature individuals. Indeed, the tail is eventually resorbed entirely, but resorption is delayed, because adults of *S. bromelicola*, *S. botocudo* and *S. mirim* with tails of different lengths and lacking tails have been observed (Bokermann, 1974; Caramaschi et al., 2009). In this case, heterochrony does not affect the offset shape of adult individuals of *Sphaenorhynchus* and can, therefore, be defined as heterochronic isomorphosis (Reilly et al., 1997).

The reduction and loss of teeth in *Sphaenorhynchus* is evident, except for *S. pauloalvini* and *S. prasinus*

(Chs. 16.1 and 21.1) and might be associated with heterochronic processes. Maxillary and premaxillary teeth are absent in *S. carneus*, *S. dorisae*, *S. planicola* and *S. mirim* (Ch. 14.0), reduced in *S. botocudo*, *S. bromelicola*, *S. platycephalus* and *S. palustris* (Ch. 16.3), and inconspicuous in *S. canga* (Ch. 16.4). Other character-states that could be associated with paedomorphosis are the coexistence of both pedicellate and nonpedicellate teeth on the maxilla (Ch. 15.1: optimizes ambiguously for the sister taxon of the *S. lacteus* group); vomerine teeth nonpedicellate (Ch. 37.0: optimizes ambiguously for the sister taxon of *S. carneus*); anguloespenial and dentary without contact, in which the Meckel's cartilage is exposed (Ch. 55.1: synapomorphy of the sister taxon of *S. pauloalvini*); palatines reduced to thin ossified slivers (Ch. 40.0: *S. carneus*, *S. dorisae* and *S. mirim*); and *lamina nariochoanalis* connected to the postnasal wall (Ch. 63.0: synapomorphy of the sister taxon of *S. carneus*). Jurgens (1971) had already suggested that the latter was a neotenic condition in *Spea* (as *Scaphiopus*; Scaphiopodidae).

In addition to delayed tail resorption and dental character-states, several other character-states found in species of *Sphaenorhynchus* appear to be paedomorphic relative to the plesiomorphic states. These include: maxilla reduced posteriorly (Ch. 13.0: synapomorphy of the sister taxon of *S. pauloalvini*); dentigerous process extremely reduced (Ch. 32.0: *S. dorisae* and *S. mirim*); dentigerous process separate from the main body of the vomer (Ch. 34.0: *S. dorisae*); posterior ramus of the pterygoid extremely short, reduced to rudimentary bumps (Ch. 30.0: synapomorphy of the sister taxon of *S. pauloalvini*); maxillary and premaxillary teeth absent (Ch. 14.0: observed in *S. carneus*, *S. dorisae*, *S. planicola* and *S. mirim*), and extreme reduction of premaxillary and maxillary teeth (Ch. 16.3: maxilla edentate across 55–80% of its length in *S. botocudo*, *S. bromelicola*, *S. palustris* and *S. platycephalus*; 16.4: maxilla edentated across 95% of its length in *S. canga*; and Ch. 21.0: part of *pars dentalis* of premaxilla edentate in *S. botocudo*, *S. cammaeus* and *S. canga*, for example).

Outside *Sphaenorhynchus*, some species of *Pseudis* (*P. paradoxa* and *P. platensis*) show a shift in the timing of sexual maturity (Downie et al., 2009; Fabrezi et al., 2010). *Pseudis platensis* shows delayed metamorphosis (with a low rate of development), in which the events related to the loss of the vent tube and resorption of the tail are postdisplaced, taking place after the larval mouth structures have disappeared and the skull transformations are complete (Fabrezi and Quinzio, 2008).

Oviposition site

Previous studies have focused on the description of external morphology of adults and larvae of *Sphaenorhynchus* (e.g. Lutz and Lutz, 1938; Bokermann, 1966, 1973), and limited information is available on their biology, reproduction and behaviour of adults and larvae (Bokermann, 1966; Suárez-Mayorga and Lynch, 2001).

Adults of *Sphaenorhynchus* are known to inhabit mainly open areas (temporary, permanent or semi-permanent ponds), where males vocalize while perched on the floating vegetation or partially submerged in water, or more rarely perched on bushes (e.g. Lutz and Lutz, 1938; Bokermann, 1973; Cruz and Peixoto, 1980; C.F.B. Haddad, pers. obs.). There are no records of oviposition site for *S. botocudo*, *S. bromelicola*, *S. mirim*, *S. palustris*, *S. platycephalus* and *S. prasinus* (Lutz and Lutz, 1938; Bokermann, 1966, 1973, 1974; Heyer et al., 1990; Toledo et al., 2007; Caramaschi et al., 2009).

Sphaenorhynchus caramaschii, *S. dorisae*, *S. lacteus*, *S. planicola* and *S. surdus*[1] lay their eggs in water, attached to submerged vegetation (Ch. 191.2; Cruz, 1973; Rodriguez and Duellman, 1994; Reichle and Köhler, 1998; Duellman, 2005; Izecksohn and Carvalho-e-Silva, 2001; K. Araujo-Vieira and T. Grant, pers. obs.); *S. pauloalvini* lays its eggs on leaves out of water (Bokermann, 1973). The oviposition in *S. carneus* has been reported to occur on leaves out of water (Bokermann, 1973; as *Sphaenorhynchus habra* [sic]) or in water, attached to submerged vegetation (Crump, 1974; W. Hödl, pers. comm.). We consider it polymorphic for coding purposes (Ch. 191.0 and 191.2); further, several studies have demonstrated that the same species can display behavioural plasticity with respect to reproductive modes (e.g. *Dendropsophus ebraccatus*, *Boana pardalis* (Hylidae), *Physalaemus spiniger* (Leptodactylidae); Haddad and Pombal, 1998; Haddad and Prado, 2005; Touchon and Warkentin, 2008; Moura et al., 2011; Toledo et al., 2012) and that the existence of alternative reproductive strategies might have evolved either due to trait selection in order to maximize fitness and avoid predation and competition or in relation to specific environmental conditions (e.g. Magnusson and Hero, 1991; Haddad and Prado, 2005; Taborsky et al., 2008; Taborsky and Brockmann, 2010). The optimization of oviposition site on our TE results indicates that oviposition in water (Ch. 191.2) is plesiomorphic in *Sphaenorhynchus*, whereas oviposition on leaves out of water (Ch. 191.0) is an autapomorphy of *S. pauloalvini*. Furthermore, our hypothesis predicts that all species for which

[1]K. Araujo-Vieira and T. Grant (unpubl. data) observed a single event of oviposition by *S. surdus* in a large bromeliad directly above the water of a swamp at Torres, Rio Grande do Sul, Brazil. Although this is suggestive of polymorphism, as occurs in *S. carneus*, we prefer to await other observations to ensure that the event we observed was not merely a behavioural anomaly.

oviposition is unknown will be found to oviposit in water.

Conclusions

Our dataset for the study of the phylogenetic relationships of *Sphaenorhynchus* included 193 phenotypic characters from adult and larval morphology, osteology, myology and reproductive biology, and DNA sequences for three mitochondrial and three nuclear loci for 43 terminals of 15 ingroup species, and 12 outgroup taxa. Our results recover the monophyly of *Sphaenorhynchus* with high support, obtaining three characteristic clades that we recognize as species groups (the *S. lacteus*, *S. planicola* and *S. platycephalus* groups). Most conflict among equally parsimonious topologies is restricted to relationships inside the *S. platycephalus* group, where one of the two species for which we lack sequence data (*S. bromelicola*) exhibits wildcard behaviour. Differences in our assessment of synapomorphies of *Sphaenorhynchus* with earlier studies (Duellman and Wiens, 1992; Faivovich et al., 2005) resulted from limitations in the taxonomic sampling of those studies, which did not include *S. pauloalvini*, the sister species of the remainder of the genus.

Our study of phenotypic characters identified a number of transformations that are congruent with the occurrence of heterochronic events during the evolution of these frogs and corroborate earlier observations of precocious sexual maturity in metamorphic individuals of some species in the *S. planicola* and *S. platycephalus* groups (Bokermann, 1974; Haddad and Prado, 2005; Caramaschi et al., 2009). Our well-supported phylogenetic hypothesis will provide an evolutionary context for the study of this poorly known phenomenon and several related character systems (e.g. morphology of the larval nostril and spiracle, vocalizations; Toledo et al., 2014; Araujo-Vieira et al., 2015a).

Acknowledgments

For access to collections, and specimen and/or tissue loans we thank José M. Padial (AMNH), Denise C. Rossa-Feres (DZSJRP), Santiago Castroviejo-Fisher, Glaucia M.F. Pontes, and Camila Both (MCP-PUCRS), Magno V. Segalla and Julio Cesar de Moura Leite (MHNCI), José P. Pombal Jr. (MNRJ), Mirco Solé (MZUESC), Marcelo F. Napoli (MZUFBA), Renato N. Feio (MZUFV), Camila Rabello Rievers (then at PUC Minas), Miguel Trefaut Rodrigues and Vanessa K. Verdade (USP), the late Paulo E. Vanzolini and Hussam Zaher (MZUSP), Steffen Reichle (then at The Nature Conservancy, Bolivia), Igor Joventino Roberto (UFAM), Hélio Ricardo da Silva (UFRRJ), João V. Lacerda and Paulo C.A. Garcia (UFMG), Laura Verrastro (UFRGS), Robson W. Ávila (URCA-H), Mike G. Rutherford (UWIZM), Natan Maciel (ZUFG) and Felipe Toledo (ZUEC). Walter Hödl and Steffen Reichle kindly answered our queries regarding biology of some species. Denis Jacob Machado assisted us with the use of YBYRÁ. Agustín Elias-Costa generously executed Fig. S12. Carlos Eduardo Costa-Campos, Felipe S.F. Leite, Igor Joventino Roberto, João Luiz Gasparini and Miguel Trefaut Rodrigues generously allowed us to use their photos. For support in different stages of this research, we thank: Glaucia M.F. Pontes, Roberto E. Reis, Patrick Colombo, Raquel R. Santos, Mauricio Rivera-Correa, Marco Rada, Danielle A. Fabri and Mariangeles A. Hernandez (Laboratório de Sistemática de Vertebrados-PUCRS); Bianca v. M. Berneck and Victor G. D. Orrico (Departamento de Zoologia, UNESP); and Martin O. Pereyra, Andrés Brunetti, Laura Nicoli, Sebastián Barrionuevo, Carlos Taboada, M. Celeste Luna, Agustín Elias-Costa and Daiana Ferraro (Divisón Herpetología, MACN). Financial support and fellowships were provided by São Paulo Research Foundation (FAPESP procs. #2012/10000-5, #2013/20423-3, #2013/50741-7, and #2014/50342-8), Agencia Nacional de Promoción Científica y Tecnológica (ANPCyT, PICT 404/2013 and 820/2015), Conselho Nacional de Desenvolvimento Científico e Tecnológico (CNPq) and Organización de los Estados Americanos (OEA).

References

Altig, R., McDiarmid, R.W., 1999. Body plan. Development and morpohology. In: Altig, R., McDiarmid, R.W. (Eds.) Tadpoles. The Biology of *Anuran Larvae*. University of Chicago Press, Chicago, IL, pp. 29–51.

Araujo-Vieira, K., Tacioli, A., Faivovich, J., Orrico, V.G.D., Grant, T., 2015a. The tadpole of *Sphaenorhynchus caramaschii*, with comments on larval morphology of *Sphaenorhynchus* (Anura: Hylidae). Zootaxa 3904, 270–282.

Araujo-Vieira, K., Lacerda, J.V.A., Pezzuti, T.L., Leite, F.S., Assis, C.L., Cruz, C.A.G., 2015b. A new species of hatchet-faced treefrog *Sphaenorhynchus* Tschudi (Anura: Hylidae) from Quadrilátero Ferrífero, Minas Gerais, southeastern Brazil. Zootaxa 4059, 96–114.

Araujo-Vieira, K., Caramaschi, U., Grillitsch, H., Grant, T., Faivovich, J., 2018. On the identity of *Sphaenorhynchus platycephalus* (Werner, 1894) (Anura: Hylidae). S. Am. J. Herpetol. 13, 73–84.

Barrio, A., 1965. Cloricia fisiologica en batracios anuros. Physis. 69, 137–142.

Barrio-Amorós, C.L., Pascual, A.D., Mueses-Cisneros, J.J., Infante, E., Chacón, A., 2006. *Hyla vigilans* Solano, 1971, a second species for the genus *Scarthyla*, redescription and distribution in Venezuela and Colombia. Zootaxa 1349, 1–18.

Benício, R.A., Silva, G.R., Fonseca, M.G., 2011. Amphibia, Anura, Hylidae, *Sphaenorhynchus lacteus* (Daudin, 1800): First record of the genus and species for the state of Piauí, Brazil. Check List 7, 196–197.

Bokermann, W.C.A., 1966. Duas novas espécies de "*Sphaenorhynchus*" (Amphibia, Hylidae). Rev. Brasil. Biol. 26, 15–21.

Bokermann, W.C.A., 1973. Duas novas espécies de "*Sphaenorhynchus*" da Bahia (Anura, Hylidae). Rev. Brasil. Biol. 33, 589–594.

Bokermann, W.C.A., 1974. Observações sobre desenvolvimento precoce em *Sphaenorhynchus bromelicola* Bokermann, 1966 (Anura, Hylidae). Rev. Brasil. Biol. 36, 33–41.

Bremer, K., 1988. The limits of amino acid sequence data in angiosperm phylogenetic reconstruction. Evolution 42, 795–803.

Burton, T.C., 1996. Adaptation and evolution in the hand muscles of Australo-Papuan hylid frogs (Anura: Hylidae: Pelodryadinae). Aust. J. Zool. 44, 611–623.

Burton, T.C., 1998. Variation in the hand and superficial throat musculature of neotropical leptodactyloid frogs. Herpetologica 54, 53–72.

Burton, T.C., 2004. Muscles of the pes of hylid frogs. J. Morphol. 260, 209–233.

Caramaschi, U., 2010. Descrição do girino de *Sphaenorhynchus surdus* (Cochran, 1953) (Anura, Hylidae). Bol. Mus. Biol. Mello Leitão, Nova Sér. 27, 67–74.

Caramaschi, U., Almeida, A.P., Gasparini, J.L., 2009. Description of two new species of *Sphaenorhynchus* (Anura, Hylidae). Zootaxa 2115, 34–46.

Cochran, D.M., 1953. Three new Brazilian frogs. Herpetologica 8, 111–115.

Crump, M.L., 1974. Reproductive strategies in a tropical anuran community. Misc. Publ. Mus. Nat. Hist. Univ. Kans. 61, 1–65.

Cruz, C.A.G., 1973. Observações sobre o girino de *Sphaenorhynchus planicola* (Lutz & Lutz, 1938) (Amphibia, Anura, Hylidae). Arq. Mus. Nac. Rio de J. 3, 83–86.

Cruz, C.A.G., Peixoto, O.L., 1980. Notas sobre o girino de *Sphaenorhynchus orophilus* (Lutz & Lutz, 1938) (Amphibia, Anura, Hylidae). Rev. Brasil. Biol. 40, 383–386.

Daudin, F.M., 1800. Histoire Naturelle des Quadrupèdes Ovipares. Livraison 2. Marchant et Cie, Paris.

Downie, J.R., Sams, K., Walsh, P.T., 2009. The paradoxical frog *Pseudis paradoxa*: Larval anatomical characteristics, including gonadal maturation. Herpetol. J. 19, 1–10.

Duellman, W.E., 1974. A reassessment of the taxonomic status of some neotropical hylid frogs. Occ. Pap. Mus. Nat. Hist. Univ. Kans. 27, 1–27.

Duellman, W.E., 1978. The biology of an equatorial herpetofauna in Amazonian Ecuador. Misc. Publ. Mus. Nat. Hist. Univ. Kans. 65, 1–352.

Duellman, W.E., 2001. Hylid Frogs of Middle America. Soc. Study Amphibians Rep., Contribut. Herpetol. 18:1–1158.

Duellman, W.E., 2005. Cusco Amazónico. The Lives of Amphibians and Reptiles in an Amazonian Rainforest. Cornell University Press, Ithaca, NY, xv + 433 pp.

Duellman, W.E., Wiens, J.J., 1992. The status of the hylid frog genus *Ololygon* and the recognition of *Scinax* Wagler, 1830. Misc. Publ. Mus. Nat. Hist. Univ. Kans. 15, 1–23.

Duellman, W.E., Marion, A.M., Hedges, S.B., 2016. Phylogenetics, classification, and biogeography of the treefrogs (Amphibia: Anura: Arboranae). Zootaxa 4104, 1–109.

Dunlap, D.G., 1960. The comparative myology of the pelvic appendage in the Salientia. J. Morphol. 106, 1–76.

Fabrezi, M., 1992. El carpo de los anuros. Alytes 10 , 1–29.

Fabrezi, M., 1993. The anurans tarsus. Alytes 11 , 46–63.

Fabrezi, M., Quinzio, S.I., 2008. Morphological evolution in Ceratophryinae frogs (Anura. Neobatrachia): The effects of heterochronic changes during larval development and metamorphosis. Zool. J. Linn. Soc. 154, 752–780.

Fabrezi, M., Quinzio, S.I., Goldberg, J., 2010. The ontogeny of *Pseudis platensis* (Anura, Hylidae): Heterochrony and the effects of larval development on postmetamorphic life. J. Herpetol. 271, 496–510.

Faivovich, J., 2002. A cladistic analysis of *Scinax* (Anura: Hylidae). Cladistics 18, 367–393.

Faivovich, F., Haddad, C.F.B., Garcia, P.C.A., Frost, D.R., Campbell, J.A., Wheeler, W.C., 2005. Systematic review of the frog family Hylidae, with special reference to Hylinae: Phylogenetic analysis and taxonomic revision. Bull. Am. Mus. Nat. Hist. 294, 240.

Faivovich, J., Moravec, J., Cisneros-Heredia, D. F., Köhler, J., 2006. A new species of the *Hypsiboas benitezi* group (Anura: Hylidae) from the western Amazon basin (Amphibia: Anura: Hylidae). Herpetologica 62, 96–108.

Faivovich, J., Haddad, C.F.B., Baêta, D., Jungfer, K.H., Álvares, G.F.R., Brandão, R.A., Sheil, C.A., Barrientos, L.S., Barrio-Amorós, C.L., Cruz, C.A.G., Wheeler, W.C., 2010. The phylogenetic relationships of the charismatic poster frogs, Phyllomedusinae (Anura, Hylidae). Cladistics 26, 227–261.

Faivovich, J., Pereyra, M.O., Luna, M.C., Hertz, A., Blotto, B.L., Vásquez-Almazán, C.R., McCranie, J.R., Sánchez, D.A., Baêta, D., Araujo-Vieira, K., Köhler, G., Kubicki, B., Campbell, J.A., Frost, D.R., Wheeler, W.C., Haddad, C.F.B., 2018. On the monophyly and relationships of several genera of Hylini (Anura: Hylidae: Hylinae), with comments on recent taxonomic changes in hylids. S. Am. J. Herpetol. 13, 1–32.

Farris, J.S., Albert, V.A., Källersjö, M., Lipscomb, D., Kluge, A.G., 1996. Parsimony jackknifing outperforms neighbor-joining. Cladistics 12, 99–124.

Garcia, P.C.A., Vinciprova, G., Haddad, C.F.B., 2003. The taxonomic status of *Hyla pulchella joaquini* (Anura: Hylidae) with description of its tadpole and vocalization. Herpetologica 59, 350–363.

Goin, C.J., 1957. Status of the frog genus *Sphoenohyla* with a synopsis of the species. Caldasia 8, 11–31.

Goloboff, P.A., 1996. Methods for faster parsimony analysis. Cladistics 12, 199–220.

Goloboff, P.A., 1999. Analyzing large data sets in reasonable times: solutions for composite optima. Cladistics 15, 415–428.

Goloboff, P.A., Catalano, S.A., 2016. TNT version 1.5, including a full implementation of phylogenetic morphometrics. Cladistics 32, 221–238.

Goloboff, P.A., Farris, J.S., Nixon, K.C., 2008. TNT, a free program for phylogenetic analysis. Cladistics 24, 774–786.

Goodman, M., Olson, C.B., Beeber, J.E., Czelusniak, J., 1982. New perspectives in the molecular biological analysis of mammalian phylogeny. Acta Zool. Fenn. 169, 19–35.

Gosner, K.L., 1960. A simplified table for staging anuran embryos and larvae with notes on identification. Herpetologica 16, 183–190.

Grant, T., Kluge, A.G., 2003. Data exploration in phylogenetic inference: Scientific, heuristic, or neither. Cladistics 19, 379–418.

Grant, T., Kluge, A.G., 2008. Credit where credit is due: The Goodman-Bremer support metric. Mol. Phylogenet. Evol. 49, 405–406.

Grant, T., Kluge, A.G., 2009. Perspective Parsimony, explanatory power, and dynamic homology testing. Syst. Biodivers. 7, 357–363.

Grant, T., Frost, D.R., Caldwell, J.P., Gagliardo, J.P.R., Haddad, C.F.B., Kok, P.J.R., Means, B.D., Noonan, B.P., Schargel, W., Wheeler, W.C., 2006. Phylogenetic systematics of dart-poison frogs and their relatives (Anura: Athesphatanura: Dendrobatidae). Bull. Am. Mus. Nat. Hist. 299, 1–262.

Grant, T., Rada, M., Anganoy-Criollo, M., Batista, A., Dias, P.H., Jeckel, A.M., Machado, D.J., Rueda-Almonacid, J.V., 2017. Phylogenetic systematics of dart-poison frogs and their relatives revisited (Anura: Dendrobatoidea). S. Am. J. Herpetol. 12, S1–S90.

Haddad, C.F.B., Pombal, J.P. Jr., 1998. Redescription of *Physalaemus spiniger* (Anura: Leptodactylidae) and description of two new reproductive modes. J. Herpetol. 32, 557–565.

Haddad, C.F.B., Prado, C.P.A., 2005. Reproductive modes in frogs and their unexpected diversity in the Atlantic forest of Brazil. Bioscience 55, 207–217.

Hall, T.A., 1999. BioEdit: a user-friendly biological sequence alignment editor and analysis program for Windows 95/98/NT. Nucl. Acids. Symp. Ser. 41, 95–98.

Hawkins, J.A., Hughes, C.E., Scotland, R.W., 1997. Primary homology assessment, characters and character states. Cladistics 13, 275–283.
Heyer, W.R., Rand, A.S., Cruz, C.A., Peixoto, G.O.L., Nelson, C.E., 1990. Frogs of Boracéia. Arq. Zool. 31, 231–410.
Horton, P., 1982. Diversity and systematic significance of anuran tongue musculature. Copeia 1982, 595–602.
Izecksohn, E., 1998. Novo gênero de Hylidae brasileiro (Amphibia, Anura). Rev. Univ. Rural, Serie Ciências da Vida 18, 47–52.
Izecksohn, E., Carvalho-e-Silva, S.P., 2001. Anfíbios do município do Rio de Janeiro. Editora UFRJ, Rio de Janeiro, 158 pp.
Jungfer, K.H., Faivovich, J., Padial, J.M., Castroviejo-Fisher, S., Lyra, M.M., Berneck, B.V.M., Iglesias, P.P., Kok, P.J.R., MacCulloch, R.D., Rodrigues, M.T., Verdade, V.K., Gastello, C.P.T., Chaparro, J.C., Valdujo, P.H., Reichle, S., Moravec, J., Gvoždík, V., Gagliardi-Urrutia, G., Ernst, R., De la Riva, I., Means, D.B., Lima, A.P., Señaris, J.C., Wheeler, W.C., Haddad, C.F.B., 2013. Systematics of spiny-backed treefrogs (Hylidae: *Osteocephalus*): an Amazonian puzzle. Zool. Scr. 42, 351–380.
Jurgens, J.D., 1971. The morphology of the nasal region of amphibia and its bearing on the phylogeny of the group. Ann. Univ. Van Stellenbosch 46, 1–146.
Katoh, K., Standley, D.M., 2013. MAFFT multiple sequence alignment software version 7: improvements in performance utility. Mol. Biol. Evol. 30, 772–780.
Kearney, M., 2002. Fragmentary taxa, missing data, and ambiguity: mistaken assumptions and conclusions. Syst. Biol. 51, 369–381.
Kearney, M., Clark, J.M., 2003. Problems due to missing data in phylogenetic analyses including fossils: a critical review. J. Vertebr. Paleontol. 23, 263–274.
Kenny, J.S., 1969. The Amphibia of Trinidad. Studies Fauna Curaçao Other Caribbean Islands 108, 1–78.
Kluge, A.G., 1989. A concern for evidence and a phylogenetic hypothesis of relationships among *Epicrates* (Boidae, Serpentes). Syst. Zool. 38, 7–25.
Kluge, A.G., Grant, T., 2006. From conviction to anti-superfluity: old and new justifications for parsimony in phylogenetic inference. Cladistics 22, 276–288.
La Marca, E., Azevedo-Ramos, C., Coloma, L.A., Ron, S., Hardy, J., 2010. *Sphaenorhynchus lacteus*. The IUCN red list of threatened species.
Lacerda, J.V.A., Moura, M.R., 2013. Vocal repertoire of *Sphaenorhynchus palustris* (Anura, Hylidae), with notes on *S. botocudo*. Salamandra 49, 105–108.
Luna, M.C., McDiarmid, R.W., Faivovich, J., 2018. From erotic excrescences to pheromone shots: structure and diversity of nuptial pads in anurans. Biol. J.Linnean Soc. 124, 403–446.
Lutz, A., Lutz, B., 1938. I. On *Hyla aurantiaca* Daudin and *Sphoenorhynchus* Tschudi and on two allied Hylae from south-eastern Brasil. An. Acad. Bras. Cienc. 10, 175–194.
Machado, D.J., 2015. YBYRÁ facilitates comparison of large phylogenetic trees. BMC Bioinformatics 16, 204.
Maddison, W., Maddison, D., 2015. Mesquite: a modular system for evolutionary analysis. Version 3.03 (7 May 2015). Accessible at http://mesquiteproject.org.
Magnusson, W.E., Hero, J.M., 1991. Predation and the evolution of complex oviposition behavior in Amazon rainforest frogs. Oecologia 86, 310–318.
Moura, M.R., Motta, A.P., Feio, R.N., 2011. An unusual reproductive mode in *Hypsiboas* (Anura: Hylidae). Zoologia 28, 142–144.
Nixon, K.C., 1999. The parsimony ratchet, a new method for rapid parsimony analysis. Cladistics 15, 407–414.
Nixon, K.C., Wheeler, Q.D., 1992. Extinction and the origin of species. In: Novacek, M.J., Wheeler, Q.D. (Eds.), Extinction and Phylogeny. Columbia University Press, New York, NY, pp. 119–143.
Padial, J.M., Grant, T., Frost, D.R., 2014. Molecular systematics of terraranas (Anura: Brachycephaloidea) with an assessment of the effects of alignment and optimality criteria. Zootaxa 3825, 1–132.
Parmalee, J.R., 1999. Trophic ecology of a tropical anuran assemblage. Sci. Pap. Nat. Hist. Mus. Univ. Kans. 11, 1–59.
Pinheiro, P.D.P., Kok, P.J.R., Noonan, B.P., Means, D.B., Haddad, C.F.B., Faivovich, J., 2019. A new genus of Cophomantini, with comments on the taxonomic status of *Boana liliae* (Anura, Hylidae). Zool. J. Linn. Soc. 185, 226–245.
Pyron, R.A., 2014. Biogeographic analysis reveals ancient continental vicariance and recent oceanic dispersal in amphibians. Syst. Biol. 63, 779–797.
Pyron, R.A., Wiens, J.J., 2011. A large-scale phylogeny of Amphibia including over 2,800 species, and a revised classification of extant frogs, salamanders, and caecilians. Mol. Phylogenet. Evol. 61, 543–583.
Reichle, S., Köhler, J., 1998. Saisonale und wasserstandsabhängige Rufplatzverteilung von Froschlurchen der südlichen Beni-Savannen, Bolivien. Salamandra 34, 43–54.
Reilly, S.M., Wiley, E.O., Meinhardt, D.J., 1997. An integrative approach to heterochrony: the distinction between interspecific and intraspecific phenomena. Biol. J. Linn. Soc. 60, 119–143.
Roberto, I.J., Araujo-Vieira, K., Carvalho-e-Silva, S.P., Ávila, R.W., 2017. A new species of *Sphaenorhynchus* (Anura: Hylidae) from northeastern Brazil. Herpetologica 73, 148–161.
Rodriguez, L.O., Duellman, W.E., 1994. Guide to the frogs of the Iquitos region, Amazonian Peru. Sci. Pap. Nat. Hist. Mus. Univ. Kans. 22, i–ii. 1–80.
Ruiz-Carranza, P.M., Lynch, J.D., 1982. Dos nuevas especies de Hyla (Amphibia: Anura) de Colombia, con aportes al conocimiento de *Hyla bogotensis*. Caldasia 13, 647–671.
Sabaj, M.H., 2016. *Standard Symbolic Codes for Institutional Resource Collections in Herpetology and Ichthyology: An Online Reference*. Version 6.5 (16 August 2016). American Society of Ichthyologists and Herpetologists, Washington, DC. Available at http://www.asih.org/.
Sankoff, D., 1975. Minimal mutation trees of sequences. SIAM J. Appl. Math. 28, 35–42.
Strong, E.E., Lipscomb, D.L., 1999. Character coding and inapplicable data. Cladistics 15, 363–371.
Suaréz, P., Cardozo, D., Baldo, D., Pereyra, M.O., Faivovich, J., Orrico, V.G.D., Catroli, G.F., Grabiele, M., Bernarde, P.S., Nagamachi, C.Y., Haddad, C.F.B., Pieczarka, J.C., 2013. Chromosome evolution in Dendropsophini (Amphibia: Anura: Hylinae). Cytogenet. Genome Res. 141, 295–308.
Suárez-Mayorga, A.M., Lynch, J.D., 2001. Los renacuajos colombianos de *Sphaenorhynchus* (Hylidae), descripciones, anotaciones sistemáticas y ecológicas. Rev. Acad. Colomb. Cienc. Exactas Fis. Nat. 25, 411–420.
Taboada, C., Brunetti, A.E., Alexandre, C., Lagorio, M.G., Faivovich, J., 2017. Fluorescent frogs: A herpetological perspective. S. Am. J. Herpetol. 12 , 1–13.
Taborsky, M., Brockmann, H.J., 2010. Alternative reproductive tactics and life history phenotypes. In: Kappeler, P. (Ed.), Animal Behaviour: Evolution and Mechanisms. Springer, Heidelberg, pp. 537–586.
Taborsky, M., Oliveira, R.F., Brockmann, H.J., 2008. The evolution of alternative reproductive tactics: concepts and questions. In: Oliveira, R.F., Taborsky, M., Brockmann, H.J. (Eds.), Alternative Reproductive Tactics: An Integrative Approach. Cambridge University Press, Cambridge, UK, pp 1–21.
Taylor, W.R., Van Dyke, G.C., 1985. Revised procedures for staining and clearing small fishes and other vertebrates for bone and cartilage study. Cybium 9, 107–119.
Toledo, L.F., Garcia, P.C.A., Lingnau, R., Haddad, C.F.B., 2007. A new species of *Sphaenorhynchus* (Anura; Hylidae) from Brazil. Zootaxa 1658, 57–68.
Toledo, L.F., Garey, M.V., Costa, T.R.N., Lourenço-de-Moraes, R., Hartmann, M., Haddad, C.F.B., 2012. Alternative reproductive modes of Atlantic Forest frogs. J. Ethol. 30, 331–336.
Toledo, L.F., Llusia, D., Vieira, C.A., Corbo, M., Márquez, M., 2014. Neither convergence nor divergence in the advertisement call of sympatric congeneric Neotropical frogs. Bioacoustics 2014, 1–17.

Touchon, J.C., Warkentin, K.M., 2008. Reproductive mode plasticity: aquatic and terrestrial oviposition in a treefrog. Proc. Natl Acad. Sci. USA 105, 7495–7499.
Trewavas, E., 1933. The hyoid and larynx of the anura. Phil. Trans. R. Soc. Lond., Ser. B. 222, 401–527.
Trueb, L., 1973. Bones, frogs, and evolution. In: Vlal, J.L. (Ed.), Evolutionary Biology of the Anurans: Contemporary Research on Major Problems. University of Missouri Press, Columbia, MO, pp. 65–132.
Trueb, L., 1993. Patterns of cranial diversification among the Lissamphibia. In: Hanken, J., Hall, B.K. (Eds.), The Skull. University of Chicago Press, Chicago, IL, pp. 255–343.
Trueb, L., Tyler, M.J., 1974. Systematics and evolution of the Greater Antillean hylid frogs. Occ. Pap. Mus. Nat. Hist. Univ. Kans. 24, 1–60.
Tyler, M.J., 1971. The phylogenetic significance of vocal sac structure in hylid frogs. Occ. Pap. Mus. Nat. Hist. Univ. Kans. 19, 319–360.
Varón, A., Wheeler, W.C., 2012. The tree alignment problem. BMC Bioinformatics 13, 293.
Varón, A., Wheeler, W.C., 2013. Local search for the generalized tree alignment. BMC Bioinformatics 14, 66.
Werner, F., 1894. Über einige Novitäten der herpetologischen Sammlung des Wiener zoolog. vergl. anatom Instituts. Zool. Anz. 17, 155–157.
Wheeler, W.C., 1996. Optimization alignment: the end of multiple sequence alignment in phylogenetics?. Cladistics 12, 1–9.
Wheeler, W.C., 2003a. Iterative pass optimization of sequence data. Cladistics 19, 254–260.
Wheeler, W.C., 2003b. Implied alignment: a synapomorphy-based multiple sequence alignment method. Cladistics 19, 261–268.
Wheeler, W.C., Aagesen, L. , Arango, C.P , Faivovich, J., Grant, T., D'haese, C., Janies, D.A., Smith, W.L., Varon, A., Giribet, G., 2006. Dynamic Homology and Phylogenetic Systematics: A Unified Approach Using POY. American Museum of Natural History, New York, NY. ISBN 0-913424-58-7.
Wheeler, W.C., Lucaroni, N., Hong, L., Crowley, L.M., Varón, A., 2015. POY version 5: phylogenetic analysis using dynamic homologies under multiple optimality criteria. Cladistics 31, 189–196.
Wiens, J.J., Fetzner, J.W., Parkinson, C.L., Reeder, T.W., 2005. Hylid frog phylogeny and sampling strategies for speciose clades. Syst. Biol. 54, 719–748.
Wiens, J.J., Graham, C.H., Moen, D.S., Smith, S.A., Reeder, T.W., 2006. Evolutionary and ecological causes of the latitudinal diversity gradient in hylid frogs: treefrog trees unearth the roots of high tropical diversity. Am. Naturalist 168 , 579–596.
Wiens, J.J., Kuczynski, C.A., Hua, X., Moen, D.S., 2010. An expanded phylogeny of treefrogs (Hylidae) based on nuclear and mitochondrial sequence data. Mol. Phylogenet. Evol. 55, 871–882.

Supporting Information

Additional supporting information may be found online in the Supporting Information section at the end of the article.

Figure S1. Phylogenetic relationships of *Sphaenorhynchus* as recovered in one of the 14 most-parsimonious trees (length 751 steps) obtained from the analysis of the phenotypic dataset (PD).

Figure S2. Phylogenetic relationships of *Sphaenorhynchus* as recovered in one of the four most-parsimonious trees (length 8769 steps) obtained from the analysis of the molecular-only dataset (MD).

Figure S3. Dorsal views of the frontoparietals of (a) *Scinax alter* (MCP 1670), (b) *Sci. catharinae* (MCP 3427), (c) *Sphaenorhynchus planicola* (MNRJ 54808), (d) *S. palustris* (MNRJ 42656), (e) *S. pauloalvini* (MNRJ 4323) and (f) *Pseudis minuta* (MACN-He 43532) showing some states of characters 4, 5 and 6 (character number is followed by the state number). Scale bars = 2 mm.

Figure S4. Quadratojugal–squamosal relationship.

Figure S5. Lateral view of quadratojugal and squamosal showing states of characters 22 and 24–27 related to these bones (character number is followed by the state number).

Figure S6. Ventral view of pterygoid showing states of characters 29 and 30 related to the medial and posterior rami of this bone (character number is followed by the state number).

Figure S7. Ventral view of vomers showing states of characters 32, 34, and 39 related to this bone (character number is followed by the state number).

Figure S8. Plectral apparatus of (a) *Scinax alter* (MCP 1670), (b) *Scarthyla goinorum* (MCP 12962), (c) *Sphaenorhynchus caramaschii* (CFBH 6937), (d) *S. carneus* (ZUEC 5555) and (e) *S. pauloalvini* (MNRJ 4323).

Figure S9. Nasal cartilages of (a) *Sphaenorhynchus prasinus* (MZUESC 6861) and (b) *S. surdus* (MCP 8324). Character number is followed by the state number. Scale bars = 1 mm.

Figure S10. Ventral views of the anterior part of the larynx showing some states of character 74.

Figure S11. Ventral views of the larynx (character number is followed by the state number).

Figure S12. Lateral view of scapulae (left), and dorsal view of presacral and sacral diapophyses (right; character number is followed by the state number).

Figure S13. Subcloacal ornamentations.

Figure S14. Submandibular musculature of hyoid.

Figure S15. (a) Dorsal view of the right hand of *Sphaenorhynchus planicola* (MNRJ 54355); note two insertions of the EDCL on digiti V, one on the metacarpal V (present in all taxa), and an additional one on the fascia of the medial slip of the EBP V, reaching proximally the proximal phalanx V (Ch. 171.1); also note the presence of the m-EBD IV (Ch. 174.1).

Appendix S1. Voucher specimens, collection numbers, localities and GenBank accession numbers of mitochondrial and nuclear genes sequences employed in this study.

Appendix S2. Voucher specimens examined for phenotypic characters.

Appendix S3. Uncorrected p-distances between *16S* (AR-BR/Wilk fragment; ~570 bp) sequences of species of *Sphaenorhynchus*.

Appendix S4. Primers used to amplify and sequence DNA in this study.

Appendix S5. Phenotypic dataset employed in the cladistic analysis of *Sphaenorhynchus*.

Appendix S6. Description and analysis of phenotypic characters.

Appendix S7. List of potentially informative morphological variation in *Sphaenorhynchus*.

Appendix A

Diagnosis of Sphaenorhynchini and its internal clades

Sphaenorhynchini Faivovich et al., 2018

Diagnosis. This tribe includes only the genus *Sphaenorhynchus*; therefore, the synapomorphies that diagnose this tribe are redundant with those diagnosing that genus. The monophyly of Sphaenorhynchini is supported by molecular evidence and 25 phenotypic synapomorphies (jackknife support = 100%; GB = 90). These include narrow alary process of the premaxilla (Ch. 18.0, with instances of homoplasy in *Dendropsophus elegans* and *D. sanborni*); short zygomatic ramus of squamosal (Ch. 25.1, with instances of homoplasy in *D. elegans* and *Pseudis minuta*); moderately long posterior ramus of the pterygoid (Ch. 30.2); presence of medial portion of the anterior process of vomers (Ch. 38.0); absence of posterolateral process of the crista parotica (Ch. 45.0, with one instance of homoplasy in *P. minuta*); completely expanded *pars externa plectri* (Ch. 47.2); *pars externa plectri* directed ventrally with respect to the transversal axis of skull (Ch. 49.0, with instances of homoplasy in *D. microps*); coronoid process forming a small projection (Ch. 54.1); rectangular, anteroposteriorly expanded alary cartilage (Ch. 57.0); rectangular shape hyoglossal sinus (Ch. 68.2); presence of cartilaginous process of arytenoid supporting the frenulum in the larynx (Ch. 80.1); transverse process of presacral vertebra VI perpendicular to body axis; (Ch. 92.1, with instances of homoplasy in *D. elegans* and *D. sanborni*, *P. minuta* and *Scinax alter* + *Sci. fuscovarius* clade); dark coloured nuptial pad on finger II in males (Ch. 115.1); anteriorly directed larval nostril (Ch. 132.0); larval nostril with fleshy flanges (Ch. 133.1); presence of dark pigmentation on the ventral surface of the vent tube (Ch. 144.1); medial vent tube (Ch. 145.0, with one instance of homoplasy in *Pseudis minuta*); apical supplementary element of m. *intermandibularis* (Ch. 146.1); m. *geniohyoideus lateralis* with a single slip (Ch. 154.0); presence of Burton's ligament (Ch. 169.1, with one instance of homoplasy in species of *Scinax*); presence of m. *extensor brevis distalis digiti II* medial (Ch. 172.1); absence of supplementary slip from the Metacarpal IV of the medial slip of the m. *extensor brevis profundus digiti V* (Ch. 175.0); presence of m. *flexor ossis metatarsi II* (FM II) with origin from distal tarsal 2–3 (Ch. 177.1); presence of lateral slip of the foot m. *extensor brevis distalis digiti V* (Ch. 187.1, with one instance of homoplasy in *Sci. catharinae*); and white parietal peritoneum (Ch. 190.1).

Characterization. Small to medium-sized treefrogs (combined SVL in males 15.1–41.0 mm, females 36.0–46.0 mm) with a greenish dorsal background, translucent skin, green bones and white parietal peritoneum; pointed, rounded or protruding snout in lateral view; single, subgular vocal sac, notably distended while males calling, ventrally not reaching the pectoral region (in *Sphaenorhynchus pauloalvini* and *S. prasinus*) or enlarged reaching the pectoral fold (in the remaining species of the genus); dark or light coloured nuptial pads on finger II in males; absence or presence of tympanic membrane (present in *S. lacteus* and *S. pauloalvini*); absence or presence of dermal ornamentation (tubercles, folds and/or calcar appendages) on forearm, tarsus, elbow, heel and subcloacal region in adult males and females; absence or presence of premaxillary, maxillary and vomerine teeth; adults generally inhabit ponds in open areas and forest edges; males vocalize while perched on floating vegetation or partially submerged in the water and, more rarely, on bushes and trees; advertisement call with pulsed notes; tadpoles with subterminal oral disc; uniform or irregular size marginal papillae; labial tooth row formula 1/2–3(1), 2/3(1) or 2(2)/3(1); eyes visible ventrally; short, medium-sized or extreme long spiracle; and medial vent tube posteroventraly directed, short, entirely fused to the ventral fin and positioned under the inferior margin of the ventral fin.

Comments. Most species of *Sphaenorhynchus* have been described as being green, very likely as a result of the impregnation of a high concentration of biliverdin on their tissues (Barrio, 1965; Taboada et al., 2017). Furthermore, green bones occur in juveniles and adults of most, if not all, species of *Sphaenorhynchus* (*S. canga*, *S. caramaschii*, *S. carneus*, *S. dorisae*, *S. lacteus* and *S. platycephalus*; Lutz and Lutz, 1938; Goin, 1957; Duellman, 1974; Araujo-Vieira et al., 2015a,b). We observed that *S. surdus* also has green bones. A green coloration also has been reported in eggs of *S. carneus* before being preserved (Suárez-Mayorga and Lynch, 2001). However, a spawn of *S. lacteus* photographed by Reichle and Köhler (1998) has creamy white animal poles, as did a spawn of *S. surdus* (K. Araujo-Vieira and T. Grant, pers. obs.). Suaréz et al. (2013) reported on the chromosome morphology and some cytogenetic markers of *Sphaenorhynchus caramaschii*, *S. carneus*, *S. dorisae*, and *S. lacteus*. They noticed that *S. carneus* has an increment from the plesiomorphic 24 to 26 chromosomes. They also noticed that in *S. lacteus* there is a large euchromatic telomeric band that comprises nearly the distal half of pair 2p, which they considered as the possible origin of heterochromatic b chromosomes in *S. dorisae*. The sister taxon relation of these two species supported by our results is congruent with this explanation. Our optimal topology, however, indicates that in order to better understand chromosome evolution in *Sphaenorhynchus*, it is necessary to study karyotypes of at least *S. pauloalvini*, and of some of the other unstudied species that are important for any inference due to its phylogenetic position (e.g., *S. prasinus*, at least one species of the *S. planicola* group, and at least an additional species of the *S. platycephalus* group).

Content. One genus. *Sphaenorhynchus*, which includes 15 species, of which 12 are placed in three species groups, and three are unassigned to any group (*S. carneus*, *S. pauloalvini* and *S. prasinus*).

Distribution. Amazon and Orinoco basins of Bolivia, Brazil, Colombia, Ecuador, Peru, and Venezuela; Trinidad, Guyana, Surinam, French Guyana. Atlantic Forest of southeastern Brazil, from Pernambuco in the north to northern Rio Grande do Sul in the south.

The *Sphaenorhynchus planicola* group

Sister taxon. The poorly supported clade including *Sphaenorhynchus prasinus*, and the *S. lacteus* and *S. platycephalus* groups.

Diagnosis. The monophyly of the *S. planicola* group is supported by molecular evidence and five phenotypic synapomorphies (jackknife support = 100%; GB = 1). These includes posterior portion of the internal margins of frontoparietals widely separated at the level of the *tectum synoticum* (Ch. 5.1, with one instance of homoplasy in *Xenohyla truncata*); presence of medial projection of the posterior margin of the exoccipitalis (Ch. 7.1, with one instance of homoplasy in *Scinax perpusillus*); extremely reduced posteromedial process of the parasphenoid (Ch. 43.0, with one instance of homoplasy in *Sphaenorhynchus canga*); the posterior extension of the fold of the m. *interhyoideus* surpassing the m. *pectoralis esternalis* (Ch. 152.5, with instances of homoplasy in *Dendropsophus minutus* and *D. sanborni*); and the m. *extensor brevis superficialis digiti III* with an insertion on the third metatarsus (Ch. 185.1). Further, the combination of small SVL in males (combined SVL 15.7–24.1 mmm); snout rounded in lateral view; well-developed vocal sacs, extending

laterally and toward the posterior of the pectoral region, with lateral longitudinal folds; presence of dermal fold on elbow and round calcar appendages; subcloacal ornamentation with white dermal flap with rounded lateral margins; absence of premaxillary and maxillary teeth; and absence of dorsolateral black and white lines differentiates species of this group from other species of *Sphaenorhynchus*.

Characterization. Small greenish treefrogs (combined SVL in males 15.7–24.1 mm; Lutz and Lutz, 1938; Caramaschi et al., 2009) with large vocal sac extending laterally and reaching the level of the pectoral fold, with longitudinal folds; rounded snout in lateral view; dark coloured nuptial pads on Finger II in males; absence of tympanic membrane; dermal folds on forearm, tarsus and elbow; round calcar appendage; round subcloacal dermal flap; absence of premaxillary, maxillary and vomerine teeth; absence of dorsolateral black and white lines; presence of black canthal line in some specimens of *S. planicola*; advertisement call of *S. mirim* consists of a single pulsed note with 9–25 pulses and duration of 0.034–0.101 s; known tadpoles of *S. planicola* with subterminal oral disc; marginal papillae composed of alternating large and small papillae (large papillae about twice as large as the small ones); labial tooth row formula 2 (2)/3(1); third tooth posterior row inside the oral disc; and medium-sized spiracle (spiracle length 16–24% of body length).

Content. Two species. *Sphaenorhynchus mirim* Caramaschi et al., 2009; *S. planicola* (Lutz and Lutz, 1938).

Distribution. Coastal lowlands of the State of Rio de Janeiro and State of Espírito Santo, southeastern Brazil.

The *Sphaenorhynchus lacteus* group

Sister taxon. The poorly supported clade including *Sphaenorhynchus prasinus* and the *S. platycephalus* group.

Diagnosis. The monophyly of the *S. lacteus* group is supported by molecular evidence and four phenotypic synapomorphies (jackknife support = 100%; GB = 31). These include nonmineralized intercalary elements between ultimate and penultimate phalanges (Ch. 101.0, with some instances of homoplasy in *Dendropsophus elegans*, *Scinax*, *S. platycephalus* and *Xenohyla truncata*); the light coloured nuptial pads on finger II in males (Ch. 115.0, with several instances of homoplasy in the outgroup taxa and in *S. canga*); the postaxial webbing reaches the midlength of the second phalanx of toe IV (Ch. 131.4, with instances of homoplasy in *S. botocudo*, *S. palustris* and *S. planicola*); the branch I of the m. *petrohyoideus posterior* inserted on the base of the posteromedial process of the hyoid (Ch. 158.0, with instances of homoplasy in *D. minutus*, *Pseudis minuta* and *Sci. alter*). Further, the combination of the larger SVL in males and females (combined SVL, males 26.0–41.0 mm, females 36.0–46.0 mm); pointed or rounded snout in lateral view; moderately developed vocal sac extending to the middle of the pectoral region; presence of dermal fold on elbow and round or triangular calcar appendages; subcloacal ornamentation with white dermal flap with triangular or rounded lateral margins; and absence of dorsolateral black lines differentiates these species from other species of *Sphaenorhynchus*.

Characterization. Relatively large greenish treefrogs (combined SVL in males 26.0–41.0 mm, females 36.0–46.0 mm; Rodriguez and Duellman, 1994) with large vocal sac reaching the level of the pectoral fold, with longitudinal folds in *S. lacteus*; rounded snout in lateral view; light coloured nuptial pads on finger II in males; absence or presence of tympanic membrane (present in *S. lacteus*); dermal folds on forearm, tarsus and elbow; round (as in *S. lacteus*) or triangular (as in *S. dorisae*) calcar appendage; round (as in *S. lacteus*) or triangular (as in *S. dorisae*) subcloacal dermal flap; absence or presence of premaxillary, maxillary, and vomerine teeth (present in *S. lacteus*); absence of dorsolateral black lines; presence of black canthal and white dorsolateral lines in *S. lacteus*; advertisement calls composed of 2–26 pulsed note with duration of 0.02–0.42 s; tadpoles with subterminal oral disc; uniform size marginal papillae (as in *S. dorisae*) or composed of alternating large and small papillae (large papillae about twice as large as the small ones; as in *S. lacteus*); labial tooth row formula 2(2)/3(1) (as in *S. dorisae*) or 2/3(1) (as in *S. lacteus*); third tooth posterior row placed on the posterior labium of the oral disc (as in *S. dorisae*) or inside the oral disc (as in *S. lacteus*); and short spiracle (spiracle length 3−11% of body length).

Content. Two species. *Sphaenorhynchus dorisae* (Goin, 1957); *Sphaenorhynchus lacteus* (Daudin, 1800).

Distribution. Amazon and Orinoco basins of Bolivia, Brazil, Colombia, Ecuador, Peru, and Venezuela; Trinidad, Guyana, Surinam, French Guyana, and states of Maranhão and Piauí, northeastern Brazil.

The *Sphaenorhynchus platycephalus* group

Sister taxon. *Sphaenorhynchus prasinus*, but its sister taxon relation with the *S. platycephalus* group is poorly supported.

Diagnosis. The monophyly of the *S. platycephalus* group is supported by molecular evidence and eight phenotypic synapomorphies (jackknife support = 98%; GB = 11). These are as follows: maxilla overlapping the premaxilla (Ch. 17.1, with some instances of homoplasy in *S. lacteus*, *S. pauloalvini*, and outgroup taxa); the inferior prenasal cartilage laterally oriented (Ch. 59.1, with instances of homoplasy in *S. carneus* and *S. lacteus*); presence of a cartilaginous lamina that extends from the cartilaginous branch to the inferior margin of the oblique cartilage (Ch. 62.1, with instances of homoplasy in *S. lacteus*, *S. pauloalvini* and species of *Dendropsophus*); dorsolateral white line present (Ch. 111.1, with instances of homoplasy in *D. sanborni*, *Sci. alter* and *S. lacteus*); subcloacal ornamentation with a weak glandular dermal fold (Ch. 117.4); presence of two lateral thick and flat dermal pads on the ventral surface below de cloaca (Ch. 118.4); poorly developed and slightly crenulated dermal folds on tarsus (Ch. 123.3); and small, rounded or flattened tubercles on heel (Ch. 124.1, with instances of homoplasy in *D. microps* and *Phyllodytes luteolus*). Besides these synapomorphies, the species included in this group can be differentiated from other species of *Sphaenorhynchus* by the combination of a protruding snout in lateral view; a moderately developed vocal sac extending to the middle of the pectoral region, with lateral longitudinal folds; and the presence of canthal and dorsolateral white lines delimited below by a dorsolateral black line.

Characterization. Medium-sized greenish treefrogs (combined SVL in males 22.5–36.0 mm, females 20.0–33.0 mm; Lutz and Lutz, 1938; Bokermann, 1966; Heyer et al., 1990; Toledo et al., 2007; Caramaschi et al., 2009; Araujo-Vieira et al., 2015b; Roberto et al., 2017), with large vocal sac reaching the level of the pectoral fold, with longitudinal folds; protruding snout in lateral view; dark or light coloured nuptial pads on finger II in males; absence of tympanic membrane; presence or absence of tubercles or crenulated dermal folds on forearm, tarsus, elbow and heel; presence of many enlarged tubercles (as in *S. platycephalus*) or white, glandular subcloacal dermal fold; presence of premaxillary, maxillary and vomerine teeth; presence of canthal and dorsolateral white lines delimited below by a canthal and dorsolateral black lines; advertisement calls composed of 1–43 pulsed notes with duration of 0.008–10.21 s; tadpoles with uniform size marginal papillae (as in *S. bromelicola*, *S. platycephalus* and *S. surdus*) or composed of alternating large and small papillae (large papillae about twice as large as the small ones; as in *S. caramaschii*, *S. canga* and *S. palustris*); labial tooth row formula 2(2)/3(1); third posterior tooth row inside the oral disc; short (as in

S. caramaschii), medium-sized (as in *S. bromelicola*, *S. canga*, *S. platycephalus* and *S. surdus*) or large-sized spiracle (as in *S. palustris*).

Content. Eight species. *Sphaenorhynchus botocudo* Caramaschi et al., 2009; *S. bromelicola* Bokermann, 1966; *S. cammaeus* Roberto et al., 2017; *S. canga* Araujo-Vieira et al., 2015b; *S. caramaschii* Toledo et al., 2007; *S. palustris* Bokermann, 1966; *S. platycephalus* (Werner, 1894); *S. surdus* (Cochran, 1953).

Distribution. Atlantic Forest of southeastern Brazil, from Pernambuco in the north to northern Rio Grande do Sul in the south.